K-SHELL AUGER AND X-RAY RATES, TRANSITION ENERGIES, AND FLUORESCENCE YIELDS FOR MULTIPLY IONIZED NEON, OXYGEN, AND NITROGEN

by

MICHAEL A. HEIN

B.S., University of Tulsa, 1969

A MASTER'S THESIS

submitted in partial fulfillment of the

requirement for the degree

MASTER OF SCIENCE

Department of Physics

KANSAS STATE UNIVERSITY
Manhattan, Kansas

1973

Approved by:

C. P. Bhalla

Major Professor

THIS BOOK CONTAINS NUMEROUS PAGES WITH THE ORIGINAL PRINTING BEING SKEWED DIFFERENTLY FROM THE TOP OF THE PAGE TO THE BOTTOM.

THIS IS AS RECEIVED FROM THE CUSTOMER.

TABLE OF CONTENTS

PAGE

LIST OF TABLES ii

LIST OF FIGURES vi

CHAPTER

I. INTRODUCTION 1

II. THEORY 5

A. Bound State and Continuum Wavefunctions 5

B. Transition Rates 6

C. Transition Energies 9

III. NUMERICAL RESULTS 10

IV. COMPARISON WITH STATISTICAL PROCEDURE 27

V. COMPARISON WITH EXPERIMENT 37

VI. DISCUSSION AND CONCLUSIONS 39

REFERENCES 40

APPENDICES

A. CALCULATION OF TOTAL ENERGY 46

References for Appendix A 52

B. CASCADE EFFECTS ON THE FLUORESCENCE YIELD 80

References for Appendix B 82

ACKNOWLEDGEMENTS 83

ABSTRACT

LIST OF TABLES

TABLE — PAGE

I. X-ray and Auger energy shifts in eV from the normal configuration of neon ($1s^1 2s^2 2p^6$), calculated with the adiabatic method, for various configurations of neon ($1s^{\ell} 2s^m 2p^n$)..... 11

II. Single hole K-shell Auger rates $x10^4$/a.u., x-ray rates $x10^4$/a.u., and fluorescence yields for various configurations of neon ($1s^1 2s^m 2p^n$)..... 14

III. Double hole K-shell Auger rates $x10^4$/a.u., x-ray rates $x10^4$/a.u., and fluorescence fields for various configurations of neon ($1s^o 2s^m 2p^n$)..... 16

IV. X-ray and Auger energy shifts in eV from the normal configuration of oxygen ($1s^1 2s^2 2p^4$), calculated with the adiabatic method, for various configurations of oxygen ($1s^{\ell} 2s^m 2p^n$)..... 18

V. Single hole K-shell Auger rates $x10^4$/a.u., x-ray rates $x10^4$/a.u., and fluorescence yields for various configurations of oxygen ($1s^1 2s^m 2p^n$)..... 20

VI. Double hole K-shell Auger rates $x10^4$/a.u., x-ray rates $x10^4$/a.u., and fluorescence yields for various configurations of oxygen ($1s^o 2s^m 2p^n$)..... 21

VII. X-ray and Auger energy shifts in eV from the normal configuration of nitrogen ($1s^1 2s^2 2p^3$), calculated with the adiabatic method, for various configurations of nitrogen ($1s^{\ell} 2s^m 2p^n$)... 23

LIST OF TABLES (continued)

TABLE PAGE

VIII. Single hole K-shell Auger rates $x10^4$/a.u., x-ray rates $x10^4$/a.u., and fluorescence yields for various configurations of nitrogen ($1s^1 2s^m 2p^n$)..... 25

IX. Double hole K-shell Auger rates $x10^4$/a.u., x-ray rates $x10^4$/a.u., and fluorescence yields for various configurations of nitrogen ($1s^o 2s^m 2p^n$)..... 26

APPENDIX A

I. Calculated H.F. binding energy, kinetic energy, nuclear interaction energy, electron-electron interaction energy in Rydbergs, and <r> in Angstroms for neon with configuration ($1s^2 2s^2 2p^n$)..... 53

II. Calculated H.F. binding energy, kinetic energy, nuclear interaction energy, electron-electron interaction energy in Rydbergs, and <r> in Angstroms for neon with configuration ($1s^2 2s^1 2p^n$)..... 56

III. Calculated H.F. binding energy, kinetic energy, nuclear interaction energy, electron-electron interaction energy in Rydbergs, and <r> in Angstroms for neon with configuration ($1s^2 2s^o 2p^n$)..... 58

IV. Calculated H.F. binding energy, kinetic energy, nuclear interaction energy, electron-electron interaction energy in Rydbergs, and <r> in Angstroms for neon with configuration ($1s^1 2s^2 2p^n$)..... 60

LIST OF TABLES (continued)

TABLE PAGE

V. Calculated H.F. binding energy, kinetic energy, nuclear interaction energy, electron-electron interaction energy in Rydbergs, and <r> in Angstroms for neon with configuration ($1s^1 2s^1 2p^n$)..... 62

VI. Calculated H.F. binding energy, kinetic energy, nuclear interaction energy, electron-electron interaction energy in Rydbergs, and <r> in Angstroms for neon with configuration ($1s^1 2s^o 2p^n$)..... 64

VII. Calculated H.F. binding energy, kinetic energy, nuclear interaction energy, electron-electron interaction energy in Rydbergs, and <r> in Angstroms for neon with configuration ($1s^o 2s^2 2p^n$)..... 66

VIII. Calculated H.F. binding energy, kinetic energy, nuclear interaction energy, electron-electron interaction energy in Rydbergs, and <r> in Angstroms for neon with configuration ($1s^o 2s^1 2p^n$)..... 68

IX. Calculated H.F. binding energy, kinetic energy, nuclear interaction energy, electron-electron interaction energy in Rydbergs, and <r> in Angstroms for neon with configuration ($1s^o 2s^o 2p^n$)..... 70

X. Total energy in Rydbergs and expectation value of r in Angstroms of all shells for various configurations of oxygen ($1s^\ell 2s^m 2p^n$)..... 72

LIST OF TABLES (continued)

TABLE PAGE

XI. Total energy in Rydbers and expectation value of r in Angstroms of all shells for various configurations of nitrogen ($1s^{\ell}\ 2s^{m}2p^{n}$) 76

LIST OF FIGURES

FIGURE PAGE

1. K-shell fluorescence yields, calculated with the HFS model (solid lines), and K-shell fluorescence yields, calculated with the statistical model (dashed lines), versus the number of 2p-shell electrons for various configurations of neon.... 29
2. Percent deviation between the K_α x-ray rates, calculated with the HFS model, and the K_α x-ray rates, calculated with the statistical model, versus the number of 2p-shell electrons for various configurations of neon..... 30
3. Percent deviation between the total Auger rates, calculated with the HFS model, and the total Auger rates, calculated with the statistical model, versus the number of 2p-shell electrons for various configurations of neon..... 31
4. Percent deviation between the K-shell fluorescence yield, calculated with the HFS model, and the K-shell fluorescence yield, calculated with the statistical model, versus the number of 2p-shell electrons for all configurations of neon with a single K-shell vacancy..... 32
5. Percent deviation between the K-shell fluorescence yield, calculated with the HFS model, and the K-shell fluorescence yield, calculated with the statistical model, versus the number of 2p-shell electrons for all configurations of neon with a double K-shell vacancy..... 33

LIST OF FIGURES (continued)

FIGURE PAGE

6. Percent deviation between the K_α x-ray rates, calculated with the HFS model, and the K_α x-ray rates, calculated with statistical model, versus the number of 2p-shell electrons for various configurations of oxygen..... 34
7. Percent deviation between the total Auger rates, calculated with the HFS model, and the total Auger rates, calculated with the statistical model, versus the number of 2p-shell electrons for various configurations of oxygen..... 35
8. Normalized K-shell fluorescence yields, calculated with the HFS model, versus the number of 2p-shell electrons for various configurations of oxygen. ω_o is the value of ω_K for the configuration $(1s)^1(2s)^2(2p)^4$..... 36

CHAPTER I

INTRODUCTION

The de-excitation of an atom with an inner shell vacancy can occur mainly by two independent competing processes: (a) the emission of x-rays and (b) the ejection of an Auger electron. The fluorescence yield for a particular vacancy is defined as:

$$\omega_i = \frac{\Gamma_x}{\Gamma_x + \Gamma_A}$$

where Γ_x and Γ_A are the total x-ray rate and the total Auger rate respectively. The theoretical values of Γ_x and Γ_A (and therefore ω_i) depend upon the electronic configuration of the atom with an inner shell vacancy.

When the inner shell vacancy is produced in an atom without changing the electronic configuration in other shells, the theoretical results, which have been already reported by McGuire[1], and by Bhalla and co-workers[2-3] can be used. Calculations in Ref. 1-3 are with the nonrelativistic Hartree-Fock-Slater (HFS) model and are for the K-shell, L-subshells and M-subshells. Such calculations were first performed by Rubenstein[4]. The theorectical values obtained by using the hydrogenic wavefunctions with (and without) screening parameters also appear in the literature[5-8].

The relativistic calculations of the Auger rates with the statistical Thomas-Fermi-Model[10], with the nonrelativistic HFS potential[9] and with the relativistic HFS model[11-13] have been performed for the

K-shell vacancy. The x-ray rates for the K-shell and the L-subshells were calculated by Scofield[14], and by Rosner and Bhalla[15] where the effects of retardation were included and the self consistent relativistic HFS wave-functions were used. Bhalla[16] extended these calculations for the M-subshells.

It should be noted that the calculations, referred to above whether nonrelativistic or relativistic in nature, are not appropriate when an inner shell vacancy is produced in a heavy ion collision. The reason is that several additional electrons are stripped from the atom (in addition to the creation of an inner shell vacancy) in violent heavy ion collisions. The relevant experimental data are:

a) experimental observations of the charge state distributions[17]

b) increase in the x-ray transition energies[18-24] as compared to the normal x-ray energies[25]

c) decrease in the Auger electron energies[26]

d) observations of both the satellite [19,20] and hypersatellite[27] K_{α} lines.

e) significant deviations of the experimental fluorescence yields[28,29] from the normal values[30].

In order to identify the possible electronic configurations which can lead to the shifts in the x-ray and Auger energies, the relative intensities of x-ray (for example K_{α}/K_{β}) and the satellite and hypersatellite structure, explicit calculations with a realistic atomic model are needed. The importance of such calculations become more evident by another set of experiments, where the cross section of a

particular x-ray production, $\sigma_x(E)$, is measured as a function of the bombarding energy, E of the heavy ion. Several groups[31] have reported such measurements of σ_x for a range of incident energies and combinations of projectiles and target materials. The theoretical models[32-36] predict the cross section of creating a vacancy, $\sigma_I(E)$. The comparison of the theoretical $\sigma_I(E)$ can be made with $\sigma_x(E)/\omega_i$, where ω_i is the appropriate fluorescence yield which depends on the relevant electronic configuration before the de-excitation of the vacancy occurs.

Recently Larkins[37], has estimated the effects on ω_K and ω_{2p} of argon, due to alterations of the electronic configuration. This was done by using scaling factors to the x-ray and the Auger rates as calculated for the normal argon configuration with only one vacany. Fortner et al.[38] have reported similar calculations for copper. The above-mentioned procedure, which is extremely simple to use, ignores the effects which arise from the change in the bound state wave-functions, as electrons are removed from the normal configuration. Bhalla and Walters[39] have explicitly calculated for several configurations of argon, the x-ray rates, the Auger rates and the fluorescence yields. Significant deviations between the statistical scaling procedure[37] and the explicit calculations[39] were found for several cases in argon.

It is the purpose of this thesis to present theoretical x-ray rates, Auger rates and K-shell fluorescence yields for multiply ionized neon, oxygen and nitrogen, and to critically examine the approximate statistical scaling procedure for these elements.

Chapter II contains a description of the theoretical model used in the present calculations, followed by the numerical results in

Chapter III. A comparison with the statistical scaling procedure and the experimental data appears in Chapter IV. A discussion and conclusions are presented in Chapter VI.

CHAPTER II

THEORY

The one-electron bound-state wave-functions and continuum wave-functions are defined below. These are used in calculation of the x-ray and Auger transition rates. Atomic units ($\hbar = m_e = e = 1$) are used throughout.

A. Bound-State and Continuum Wave-Functions

The one-electron wave-functions are solutions of the Schrodinger equation,

$$\left[-\tfrac{1}{2} \nabla^2 + V(r) - \epsilon \right] \phi(\vec{r}) = 0 \qquad (1)$$

The spherically symmetric potential, V(r), experienced by the electron of interest, is specified for an atom of proton number Z and electron occupation numbers $N(n,\ell)$. The total number of electrons in a particular configuration is $Z_o = \sum_{n,\ell} N(n,\ell)$. This potential is defined as,

$$V(r) \equiv \begin{cases} V'(r) & , -V'(r) > (Z - Z_o + 1)/r \\ -(Z - Z_o + 1)/r & , -V'(r) \leq (Z - Z_o + 1)/r \end{cases}$$

where

$$V'(r) \equiv V_d(r) + V_x(r)$$

the direct term being

$$V_d(r) \equiv -Z/r + \int d^3r' \frac{\rho(r')}{|\vec{r} - \vec{r}'|} \quad ,$$

and the exchange term being

$$V_x(r) \equiv -2\left[\frac{3\rho(r)}{8\pi}\right]^{1/3}\left[1+\tanh(G)\right]$$

where G is an inhomogeneity term given by,

$$G \equiv \beta\left[2\left(\frac{\nabla\rho}{\rho}\right)^2 - 3\nabla^2\rho/\rho\right]/\rho^{2/3} \quad .$$

The optimum choice for β , suggested by Herman and Schwarz[40], is $\beta = 0.0028$. All of the above equations depend on a density ρ , which is defined as

$$4\pi r^2\rho(r) \equiv \sum_{n,\ell} N(n,\ell)\,P_{n\ell}^2(r)$$

wherein the wave function , $\phi(\vec{r})$, is separated as

$$\phi_{n\ell m}(\vec{r}) = P_{n\ell}(r)\,Y_{\ell m}(\hat{r})/r \quad .$$

B. Transistion Rates

Consider one inner shell vacancy designated by $n_3\,\ell_3$ in an atom with proton number Z and N electrons. Ignoring the spin-orbit coupling term, the Hamiltonian can be written as,

$$H = H_o + H'$$

where

$$H_o = \sum_{i=1}^{N}\left[-\tfrac{1}{2}\nabla_i^2 - Z/r_i + V(r_i)\right]$$

$$H' = \sum_{i<j}\frac{1}{r_{ij}} - \sum_i V(r_i)$$

The total Auger transition rate from an initial state ϕ_i to a

final state ϕ_f is

$$\Gamma_A = 2\pi \mathcal{S} |\langle \phi_f(1,2,\ldots N) | \sum_{i<j} \frac{1}{r_{ij}} | \phi_i(1,2,\ldots N) \rangle|^2$$

where $\mathcal{S}$ means average over the initial states and sum over the final states.

It is more convenient to express this total Auger rate, Γ_A, as a sum of various possible Auger group rates, T_A. The initial state is described by two electrons with quantum lables $n_1 \ell_1$ and $n_2 \ell_2$, and in the final state, one of these electrons has filled the vacancy $n_3 \ell_3$, and the other, denoted by E ℓ_4, has been ejected into the continuum. Then,

$$T_A(n_1\ell_1, n_2\ell_2 \rightarrow n_3\ell_3, E\ell_4) = 2\pi N_{12} \Sigma |\mathcal{M}|^2 \qquad (2a)$$

with

$$\mathcal{M} = \langle \phi(n_3\ell_3, E\ell_4) | \frac{1}{r_{12}} | \phi(n_1\ell_1, n_2\ell_2) \rangle \quad . \qquad (2b)$$

The ϕ's above are two-particle anti-symmetrized wave functions described by a LSJM or any other coupling scheme. The weighting factors, N_{12}, are given by,

$$N_{12} = \begin{cases} \dfrac{N_1 N_2}{(4\ell_1+2)(4\ell_2+2)} & \text{for inequivalent electrons,} \\ \dfrac{N_1(N_1-1)}{(4\ell_1+2)(4\ell_1+1)} & \text{for equivalent electrons} \\ & (N_1 = N_2,\ n_1 = n_2\ \ \ell_1 = \ell_2) \quad . \end{cases}$$

The matrix element, $\mathcal{M}$, evaluated in the LSJM coupling scheme[43], is

$$\mathcal{M} = \langle \phi(n_3\ell_3, E\ell_4, L'S'J'M' | \frac{1}{r_{12}} | \phi(n_1\ell_1, n_2\ell_2, LSJM) \rangle$$
$$= \mathcal{T}(-1)^{L+\ell_1+\ell_4} \sum_k \left[R^k(1,2,3,4) \langle \ell_3 \| C^k \| \ell_1 \rangle \times \langle \ell_4 \| C^k \| \ell_2 \rangle \right] \begin{Bmatrix} \ell_3 & \ell_4 & L \\ \ell_2 & \ell_1 & k \end{Bmatrix}$$
$$+ (-1)^{L+S} R^k(2,1,3,4) \langle \ell_3 \| C^k \| \ell_2 \rangle \times \langle \ell_4 \| C^k \| \ell_1 \rangle \begin{Bmatrix} \ell_3 & \ell_4 & L \\ \ell_1 & \ell_2 & k \end{Bmatrix} \delta_{MM'} \delta_{SS'} \delta_{JJ'} \delta_{LL'} \tag{4a}$$

with

$$\langle \ell \| C^k \| \ell' \rangle \equiv (-1)^{\ell} [(2\ell+1)(2\ell'+1)]^{1/2} \begin{Bmatrix} \ell' & k & \ell \\ 0 & 0 & 0 \end{Bmatrix} \tag{4b}$$

and

$$R^k(1,2,3,4) \equiv \int_0^\infty \int_0^\infty P_{n_1\ell_1}(r_i) P_{n_2\ell_2}(r_j) \frac{r_<^k}{r_>^{k+1}} P_{n_3\ell_3}(r_i) P_{E\ell_4}(r_j) \, dr_i \, dr_j \quad . \tag{4c}$$

The factor $\mathcal{T}$ is $\sqrt{1/2}$ if $n_1\ell_1$ and $n_2\ell_2$ are equivalent electrons; $\mathcal{T} = 1$ otherwise. The Auger group rate is now expressed as,

$$T_A(n_1\ell_1, n_2\ell_2 \rightarrow n_3\ell_3, E\ell_4) = 2\pi N_{12} \sum_J \sum_{\ell_4} \frac{(2J+1)}{2(2\ell_3+1)} |\mathcal{M}|^2 \tag{5}$$

with $\mathcal{M}$ given in (4a). The total Auger rate, Γ_A, is now the sum of all possible group rates.

The x-ray transition rate for filling a vacancy $n_3\ell_3$ and creating a vacancy $n_f\ell_f$ is given in the electric dipole approximation as,

$$T_x(n_3\ell_3 \rightarrow n_f\ell_f) = N_{3f} \, 4/3 \, k^3 \frac{\ell_>}{(2\ell_3+1)} \left| \int_0^\infty P_{n_f\ell_f} P_{n_3\ell_3} r \, dr \right|^2 \quad . \tag{6}$$

The value of k is equal to the x-ray transition energy divided by c. N_{3f} is the reduction factor given by

$$N_{3f} = \frac{N_f}{2(2\ell_f + 1)}$$ where N_f is the actual occupation number of the $n_f \ell_f$ shell.

The total x-ray rate, Γ_x, is then the sum of all possible individual transition rates given in (6). (For the elements studied here, there is only one possible transition: $2p \rightarrow 1s$).

The fluorescence yield for an initial vacancy $n_3 \ell_3$, is defined as,

$$\omega_{n_3 \ell_3} \equiv \frac{\Gamma_x}{\Gamma_x + \Gamma_A} \quad . \tag{7}$$

C. Transition Energies

The x-ray transition energies and the Auger electron energies for the initial configuration $(1s)^{\ell}(2s)^{m}(2p)^{n}$ were calculated by taking appropriate differnces between the total energies[a] of the initial and final configurations:

$$E_x(2p \rightarrow 1s) = E_{HF}(1s^{\ell} 2s^{m} 2p^{n}) - E_{HF}(1s^{\ell+1} 2s^{m} 2p^{n-1})$$

$$E_A(1s\text{-}2s\text{-}2s) = E_{HF}(1s^{\ell} 2s^{m} 2p^{n}) - E_{HF}(1s^{\ell+1} 2s^{m-2} 2p^{n})$$

$$E_A(1s\text{-}2s\text{-}2p) = E_{HF}(1s^{\ell} 2s^{m} 2p^{n}) - E_{HF}(1s^{\ell+1} 2s^{m-1} 2p^{n-1})$$

$$E_A(1s\text{-}2p\text{-}2p) = E_{HF}(1s^{\ell} 2s^{m} 2p^{n}) - E_{HF}(1s^{\ell+1} 2s^{m} 2p^{n-2}) \quad .$$

[a]See Appendix A for calculation of total energies.

CHAPTER III

NUMERICAL RESULTS

As described in Chapter II, the bound state wave-functions were calculated for all electronic configurations $(1s)^{\ell}(2s)^{m}(2p)^{n}$; ℓ=0,1, $m+n>0$ of neon with the HFS model using the HVDO exchange. The continuum wave-functions were also calculated by numerical integration of the Schrodinger equation for the appropriate Auger energies and orbital angular momentum values.

The transition energies for the 2p → 1s x-ray, and the Auger energies were calculated by the adiabatic procedure, and the energy shifts from the "normal" configuration are listed in Table I. The calculated individual Auger rates, 2p → 1s x-ray rate and the K-shell fluorescence yield are given in Table II for a single K-shell vacancy and in Table III for a double K-shell vacancy. The numerical results in these tables are for neon with configurations $(1s)^{\ell}(2s)^{m}(2p)^{n}$; ℓ=0,1, $m+n>0$.

Similar theoretical results for oxygen and nitrogen are given in Tables IV through IX. The total energies for all electronic configurations $(1s)^{\ell}(2s)^{m}(2p)^{n}$ are given in Appendix A. The indicies ℓ and m assume values of 0,1, and 2; the index n assumes values of 0 to 6 for neon, 0 to 4 for oxygen and 0 to 3 for nitrogen. Configurations from which no transition can occur are not listed.

Table I. X-ray and Auger energy shifts in eV from the normal configuration[a] of neon ($1s^2 2s^2 2p^6$), calculated with the adiabatic method, for various configurations of neon ($1s^{\ell} 2s^{m} 2p^{n}$).

Configuration			ΔE_x	ΔE_A	ΔE_A	ΔE_A
ℓ	m	n	(2p→1s)	(2s-2s)	(2s-2p)	(2p-2p)
1	2	6	0.0	0.0	0.0	0.0
1	2	5	5.2	-15.2	-17.2	-19.5
1	2	4	12.2	-30.4	-35.1	-40.4
1	2	3	20.5	-45.7	-53.8	-62.7
1	2	2	30.5	-60.9	-73.0	-86.3
1	2	1	42.2	-75.7	-92.6	--
1	1	6	6.1	--	-19.4	-16.3
1	1	5	12.4	--	-37.4	-37.0
1	1	4	20.4	--	-56.2	-59.1
1	1	3	30.0	--	-75.5	-55.0
1	1	2	41.2	--	-95.2	-106.9
1	1	1	54.1	--	-116.4	--

Table I (continued)

1	0	6	13.2	--	--	-33.6
1	0	5	20.7	--	--	-55.5
1	0	4	29.8	--	--	-78.5
1	0	3	40.5	--	--	-102.8
1	0	2	53.1	--	--	-129.2
1	0	1	65.9	--	--	--
0	2	6	96.9	68.6	67.3	65.4
0	2	5	103.8	52.6	48.3	42.9
0	2	4	112.2	36.7	28.5	19.0
0	2	3	122.2	20.8	8.1	-6.2
0	2	2	133.8	5.0	-12.9	-32.7
0	2	1	146.8	-10.6	-34.5	--
0	1	6	103.9	--	45.8	46.5
0	1	5	111.9	--	25.9	22.8
0	1	4	121.4	--	5.3	-2.3
0	1	3	132.4	--	-15.8	-28.6
0	1	2	145.0	--	-37.4	-56.2
0	1	1	159.1	--	-59.8	--

Table I (continued)

0	0	6	111.8	--	--	26.5
0	0	5	120.8	--	--	1.7
0	0	4	131.4	--	--	-24.4
0	0	3	143.5	--	--	-51.7
0	0	2	164.0	--	--	-80.5

[a] E_x (2p →1s) = 848.5eV;

E_A (2s - 2s) = 747.3eV;

E_A (2s - 2p) = 780.0eV;

E_A (2p - 2p) = 807.7eV.

Table II Single hole K-shell Auger rates x 10^4/a.u., X-ray rates x 10^4/a.u., and fluorescence yields for various configurations of neon ($1s^1 2s^m 2p^n$).

Configuration n	m	2s - 2s	2s - 2p	2p - 2p	Total Auger rate	Total X-ray rate	ω_K
6	2	8.334	24.448	55.284	88.066	1.436	0.0160
5	2	9.393	24.002	45.358	78.753	1.339	0.0167
4	2	10.701	22.507	33.070	66.278	1.194	0.0177
3	2	12.220	19.682	19.731	51.633	0.994	0.0189
2	2	13.827	15.163	7.698	36.687	0.732	0.0196
1	2	15.388	8.606	--	23.994	0.401	0.0164
6	1	--	14.150	66.278	80.428	1.596	0.0195
5	1	--	13.773	53.548	67.321	1.479	0.0215
4	1	--	12.832	38.330	51.162	1.312	0.0250
3	1	--	11.129	22.495	33.624	1.087	0.0313
2	1	--	8.442	8.670	17.113	0.796	0.0445
1	1	--	4.716	--	4.716	0.434	0.0843

Table II (continued)

6	0	--	--	77.901	77.901	1.762	0.0221
5	0	--	--	61.854	61.854	1.625	0.0256
4	0	--	--	43.571	43.571	1.435	0.0319
3	0	--	--	25.306	25.306	1.183	0.0447
2	0	--	--	9.682	9.682	0.868	0.0823
1	0	--	--	--	--	0.509	--

Table III Double hole K-shell Auger rates x 10^4/a.u., X-ray rates x 10^4/a.u., and fluorescence yields for various configurations of neon ($1s^0 2s^m 2p^n$).

Configuration n	m	2s-2s	2s-2p	2p-2p	Total Auger rate	Total X-ray rate	ω_K
6	2	10.239	33.699	85.925	129.860	2.363	0.0179
5	2	11.698	32.558	67.900	112.160	2.162	0.0189
4	2	13.390	30.020	47.598	91.009	1.893	0.0204
3	2	15.246	25.753	27.310	68.309	1.547	0.0221
2	2	17.160	19.398	10.233	46.790	1.117	0.0233
1	2	18.930	10.772	---	29.702	0.599	0.0198
6	1	---	19.192	99.936	119.128	2.611	0.0214
5	1	---	18.446	78.032	96.478	2.381	0.0241
4	1	---	16.928	54.054	70.982	2.078	0.0284
3	1	---	14.415	30.757	45.172	1.693	0.0361
2	1	---	10.726	11.475	22.201	1.219	0.0520
1	1	---	5.872	---	5.872	0.651	0.0998

Table III (continued)

6	0	---	---	116.220	116.220	2.936	0.0246
5	0	---	---	89.805	89.805	2.675	0.0289
4	0	---	---	61.849	61.849	2.336	0.0364
3	0	---	---	35.184	35.184	1.907	0.0514
2	0	---	---	13.161	13.161	1.415	0.0971
1	0	---	---	---	---	0.758	---

Table IV X-ray and Auger energy shifts in eV from the normal configuration[a] of oxygen ($1s^1 2s^2 2p^4$), calculated with the adiabatic method, for various configurations of oxygen ($1s^{\ell} 2s^{m} 2p^{n}$).

Configuration			ΔX	ΔE_A	ΔE_A	ΔE_A
ℓ	m	n	(2p→1s)	(2s-2s)	(2s-2p)	(2p-2p)
1	2	4	0.0	0.0	0.0	0.0
1	2	3	4.9	-12.1	-13.4	-16.1
1	2	2	11.5	-24.1	-27.9	-33.4
1	2	1	19.8	-35.7	-42.7	--
1	1	4	5.3	--	-15.7	-13.5
1	1	3	11.4	--	-30.4	-30.7
1	1	2	19.2	--	-45.3	-48.8
1	1	1	28.8	--	-61.7	--
1	0	4	11.8	--	--	-27.8
1	0	3	19.1	--	--	-45.7
1	0	2	28.3	--	--	-65.9
1	0	1	37.9	--	--	--

Table IV (continued)

0	2	4	78.7	54.8	53.3	51.1
0	2	3	85.2	42.1	37.5	32.0
0	2	2	93.4	29.5	21.2	11.8
0	2	1	103.1	17.1	4.4	--
0	1	4	84.8	--	35.4	35.0
0	1	3	92.5	--	19.0	14.8
0	1	2	101.5	--	2.1	-6.5
0	1	1	112.5	--	-15.6	--
0	0	4	91.9	--	--	18.0
0	0	3	100.7	--	--	-3.0
0	0	2	111.1	--	--	-25.6
0	0	1	122.5	--	--	--

[a] $E_x(2p \rightarrow 1s) = 530.5$ eV;

$E_A(2s\text{-}2s) = 463.1$ eV;

$E_A(2s\text{-}2p) = 482.8$ eV;

$E_A(2p\text{-}2p) = 498.4$ eV.

Table V Single hole K-shell Auger rates x 10^4/a.u. and X-ray rates x 10^4/a.u. and fluorescence yields for various configurations of oxygen ($1s^1 2s^m 2p^n$).

n	m	2s - 2s	2s - 2p	2p - 2p	Total Auger rate	Total X-ray rate	ω_K
4	2	8.470	16.553	22.470	47.493	0.365	0.0076
3	2	9.862	15.138	14.428	39.428	0.315	0.0079
2	2	11.538	12.228	5.980	29.746	0.240	0.0080
1	2	13.249	7.249	--	20.497	0.135	0.0065
0	2	14.821	--	--	14.821	--	--
4	1	--	9.892	28.117	38.009	0.418	0.0109
3	1	--	8.968	17.471	26.439	0.357	0.0133
2	1	--	7.100	7.070	14.170	0.269	0.0186
1	1	--	4.106	--	4.106	0.151	0.0355
4	0	--	--	33.803	33.803	0.472	0.0138
3	0	--	--	20.576	20.576	0.401	0.0191
2	0	--	--	8.242	8.242	0.302	0.0353
1	0	--	--	--	--	0.187	--

Table VI Double hole K-shell Auger rates x 10^4/a.u. and X-ray rates x 10^4/a.u. and fluorescence yields for various configurations of oxygen ($1s^o 2s^m 2p^n$).

n	m	2s - 2s	2s - 2p	2p - 2p	Total Auger rate	Total X-ray rate	ω_K
4	2	11.281	24.711	38.284	74.276	0.684	0.0091
3	2	13.288	22.037	23.011	58.336	0.572	0.0097
2	2	15.465	17.226	8.942	41.633	0.422	0.0100
1	2	17.530	9.877	--	27.407	0.230	0.0083
0	2	20.126	--	--	20.126	--	--
4	1	--	14.457	45.636	60.093	0.771	0.0127
3	1	--	12.788	26.985	39.773	0.642	0.0159
2	1	--	9.832	10.394	20.226	0.471	0.0228
1	1	--	5.518	--	5.518	0.256	0.0443

Table VI (continued)

4	0	--	--	54.467	54.467	0.895	0.0162
3	0	--	--	32.121	32.121	0.747	0.0227
2	0	--	--	12.414	12.414	0.555	0.0428
1	0	--	--	--	--	0.311	--

Table VII X-ray and Auger energy shifts in eV from the normal configuration[a] of nitrogen ($1s^1 2s^2 2p^3$), calculated with the adiabatic method, for various configurations of nitrogen ($1s^{\ell} 2s^{m} 2p^{n}$).

Configuration			ΔX	ΔE_A	ΔE_A	ΔE_A
ℓ	m	n	(2p→1s)	(2s-2s)	(2s-2p)	(2p-2p)
1	2	3	0.0	0.0	0.0	0.0
1	2	2	4.8	-10.4	-12.2	-14.3
1	2	1	11.4	-20.4	-24.7	--
1	1	3	5.0	--	-13.8	-12.0
1	1	2	11.0	--	-26.3	-27.0
1	1	1	19.0	--	-40.4	--
1	0	3	11.2	--	--	-24.4
1	0	2	18.7	--	--	-41.5
1	0	1	26.6	--	--	--
0	2	3	69.5	48.0	46.3	43.9
0	2	2	76.0	37.0	32.3	26.8
0	2	1	84.1	26.2	7.8	--

Table VII (continued)

0	1	3	75.3	--	30.3	29.3
0	1	2	82.9	--	15.9	11.1
0	1	1	92.1	--	0.6	--
0	0	3	82.1	--	--	14.0
0	0	2	90.9	--	--	-5.4
0	0	1	100.7	--	--	--

[a] $E_x(2p \rightarrow 1s) = 399.3$ eV;

$E_A(2s\text{-}2s) = 346.2$ eV;

$E_A(2s\text{-}2p) = 360.6$ eV;

$E_A(2p\text{-}2p) = 371.4$ eV.

Table VIII Single hole K-shell Auger rates x 10^4/a.u. and X-ray rates x 10^4/a.u. and fluorescence yields for various configurations of nitrogen ($1s^1 2s^m 2p^n$).

n	m	2s - 2s	2s - 2p	2p - 2p	Total Auger rate	Total X-ray rate	ω_K
3	2	8.490	12.389	11.033	31.912	0.152	0.0047
2	2	10.086	10.341	4.850	25.277	0.118	0.0046
1	2	11.836	6.345	--	18.181	0.069	0.0038
0	2	13.504	--	--	13.504	--	--
3	1	--	7.611	14.232	21.843	0.177	0.0080
2	1	--	6.220	6.003	12.223	0.136	0.0110
1	1	--	3.692	--	3.692	0.078	0.0207
3	0	--	--	17.479	17.479	0.204	0.0115
2	0	--	--	7.266	7.266	0.157	0.0212
1	0	--	--	--	--	0.101	--

Table IX Double hole K-shell Auger rates x 10^4/a.u. and X-ray rates x 10^4/a.u. and fluorescence yields for various configurations of nitrogen ($1s^0 2s^m 2p^n$).

n	m	2s - 2s	2s - 2p	2p - 2p	Total Auger rate	Total X-ray rate	ω_K
3	2	12.046	19.641	20.225	51.912	0.311	0.0060
2	2	14.348	15.790	8.088	38.226	0.233	0.0061
1	2	16.587	9.272	--	25.858	0.129	0.0050
0	2	19.459	--	--	19.459	--	--
3	1	--	11.710	24.512	36.222	0.356	0.0097
2	1	--	9.224	9.667	18.891	0.265	0.0138
1	1	--	5.274	--	5.274	0.146	0.0269
3	0	--	--	30.071	30.071	0.424	0.0139
2	0	--	--	11.901	11.901	0.320	0.0262
1	0	--	--	--	--	0.182	--

CHAPTER IV

COMPARISON WITH STATISTICAL PROCEDURE

Larkins proposed a simple approximate statistical scaling procedure to obtain the fluorescence yields for multiply ionized atoms when the theoretical x-ray and the Auger rates are available for atoms with only one inner shell vacancy. The technique, use by Larkins, and Fortner et al.[38], is to scale the individual Auger group rates and the x-ray rates, calculated only for a single inner shell vacancy, with the weighting factors (N_{ij} in eq.2) which depend upon the number of electrons in each subshell. The fluorescence yields can then be calculated for different defect configurations. This simple procedure ignores the effects on the x-ray and Auger transition energies and the wave-functions which result from the multiply ionized configurations. We present in Fig. 1 the K-shell fluorescence yield obtained from the statistical model and that of our explicit HFS calculations, for various configurations of neon. Figures 2 and 3 show the percent deviation of the statistical model from our HFS calculations, for the K_{α} x-ray rate and the total Auger rate respectively in neon. Figures 4 and 5 show the resulting percent deviation in the fluorescence yield for single and double K-shell vacancies for neon respectively. Figure 6 shows a similar deviation in the K_{α} x-ray rate for selected configurations of oxygen; Fig. 7 shows an analogous deviation in the total Auger rate for selected configurations of oxygen. The large errors, introduced by the statistical approximation are evident for most configurations. Figure 8 displays the HFS fluores-

cence yield normalized to the fluorescence yield for the "normal" configuration $(1s)^1(2s)^2(2p)^4$ of oxygen, as a function of the 2p-shell occupancy.

THIS BOOK CONTAINS NUMEROUS PAGES WITH DIAGRAMS THAT ARE CROOKED COMPARED TO THE REST OF THE INFORMATION ON THE PAGE.

THIS IS AS RECEIVED FROM CUSTOMER.

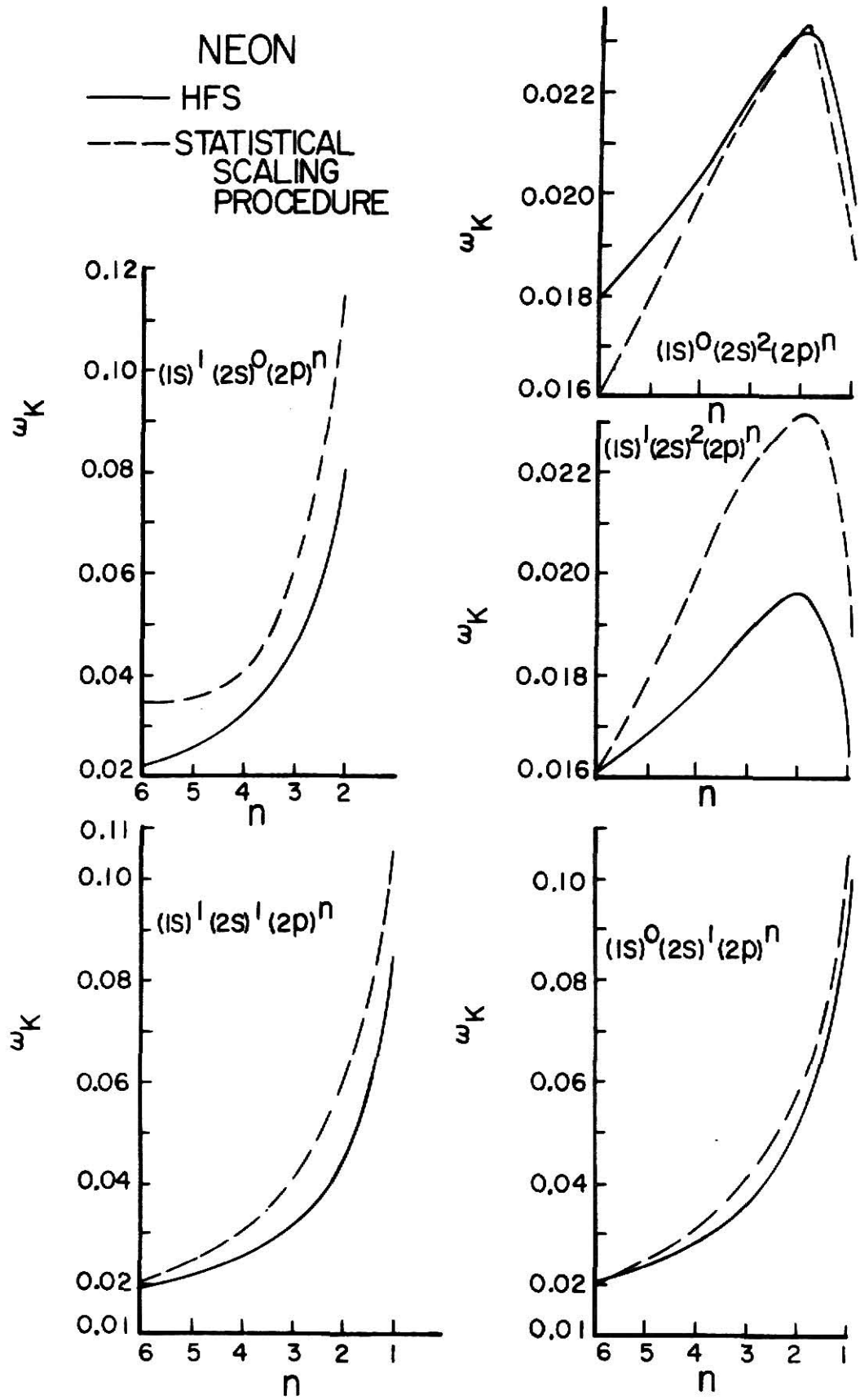

Fig. 1 K-shell fluorescence yields, calculated with the HFS model (solid lines), and K-shell fluorescence yields, calculated with the statistical model (dashed lines), versus the number of 2p-shell electrons for various configurations of neon.

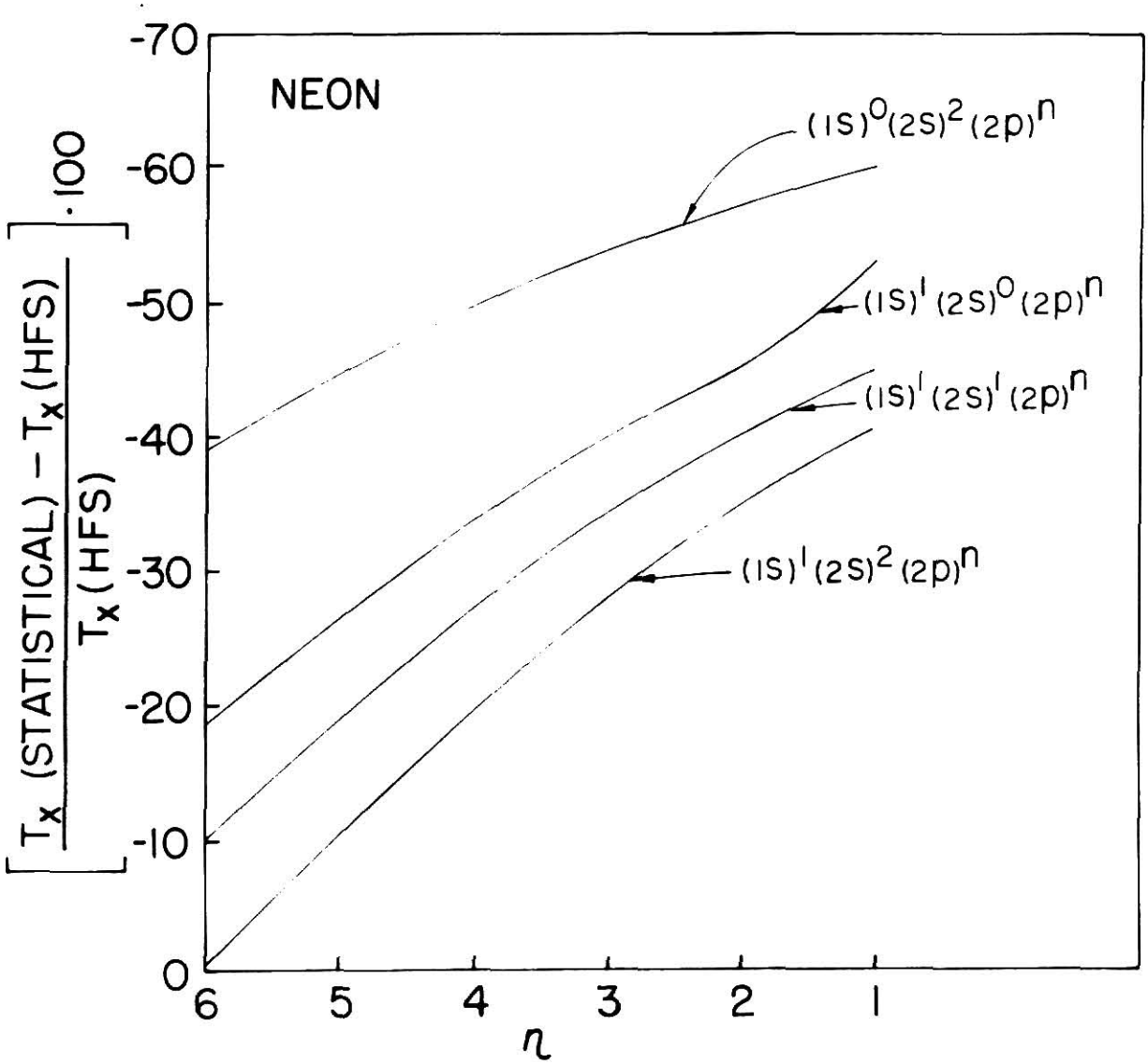

Fig. 2 Percent deviation between the K_α x-ray rates, calculated with the HFS model, and the K_α x-ray rates, calculated with the statistical model, versus the number of 2p-shell electrons for various configurations of neon.

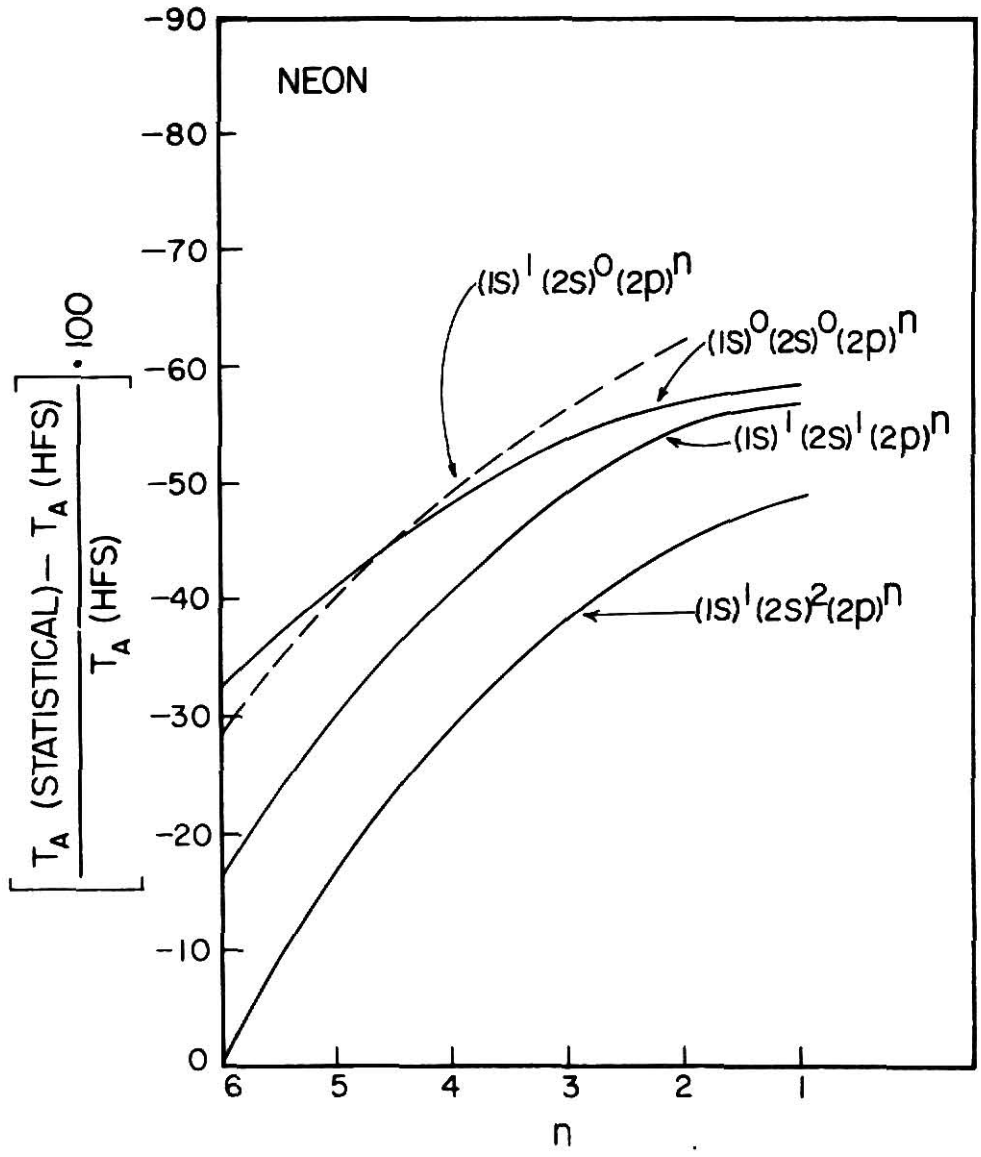

Fig. 3 Percent deviation between the total Auger rates, calculated with the HFS model, and the total Auger rates, calculated with the statistical model, versus the number of 2p-shell electrons for various configurations of neon.

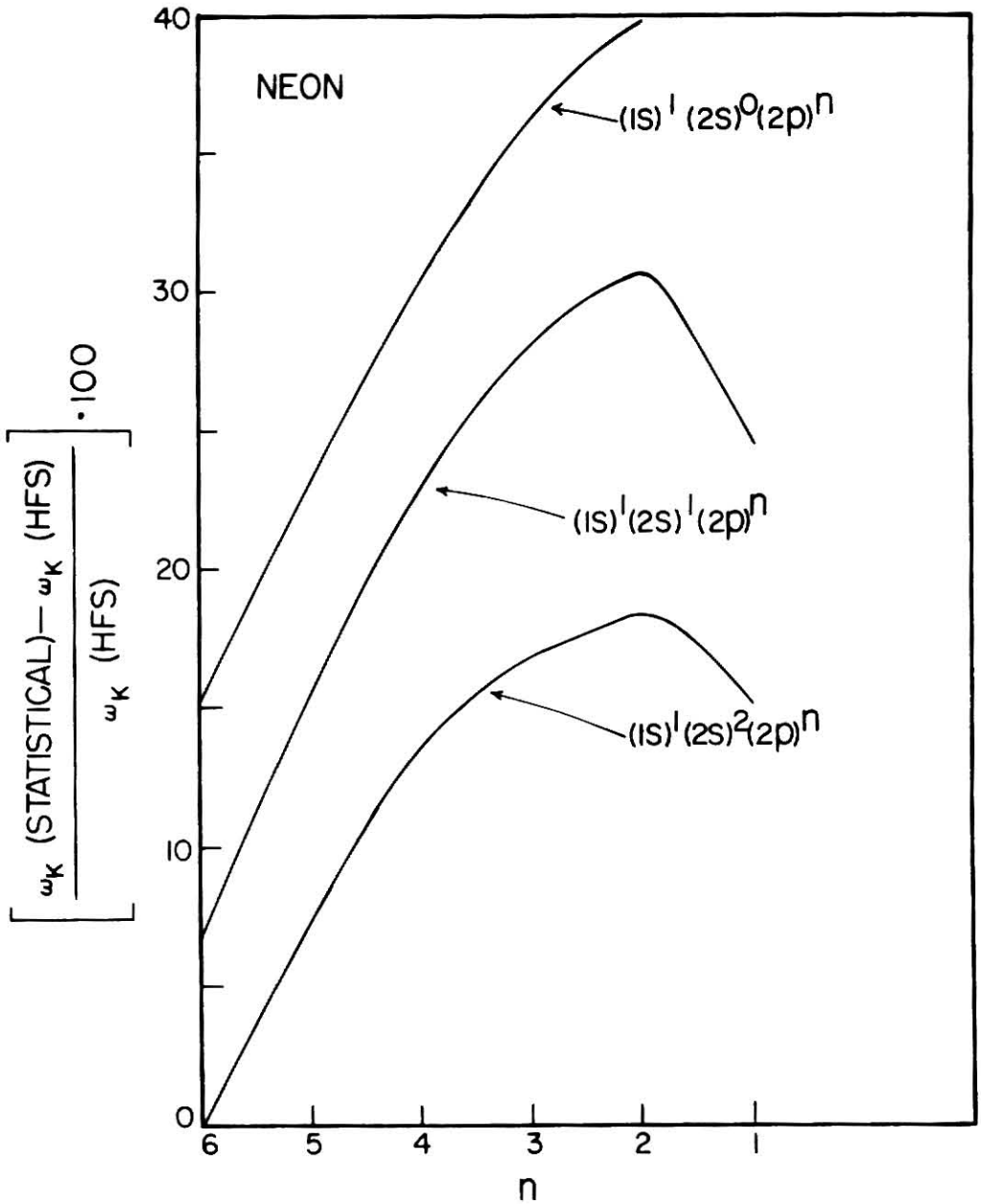

Fig. 4 Percent deviation between the K-shell fluorescence yield, calculated with the HFS model, and the K-shell fluorescence yield, calculated with the statistical model, versus the number of 2p-shell electrons for all configurations of neon with a single K-shell vacancy.

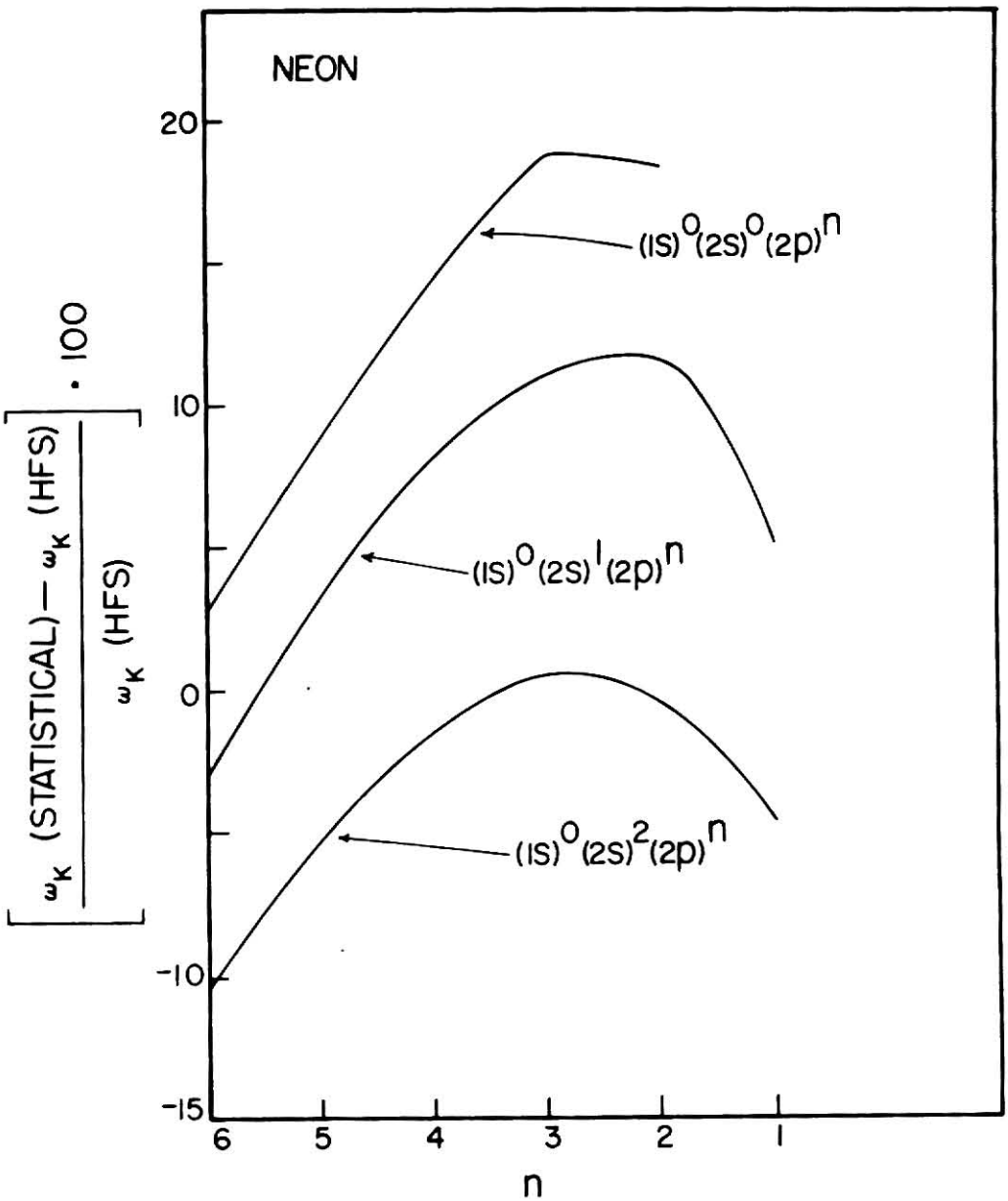

Fig. 5 Percent deviation between the K-shell fluorescence yield, calculated with the HFS model, and the K-shell fluorescence yield, calculated with the statistical model, versus the number of 2p-shell electrons for all configurations of neon with a double K-shell vacancy.

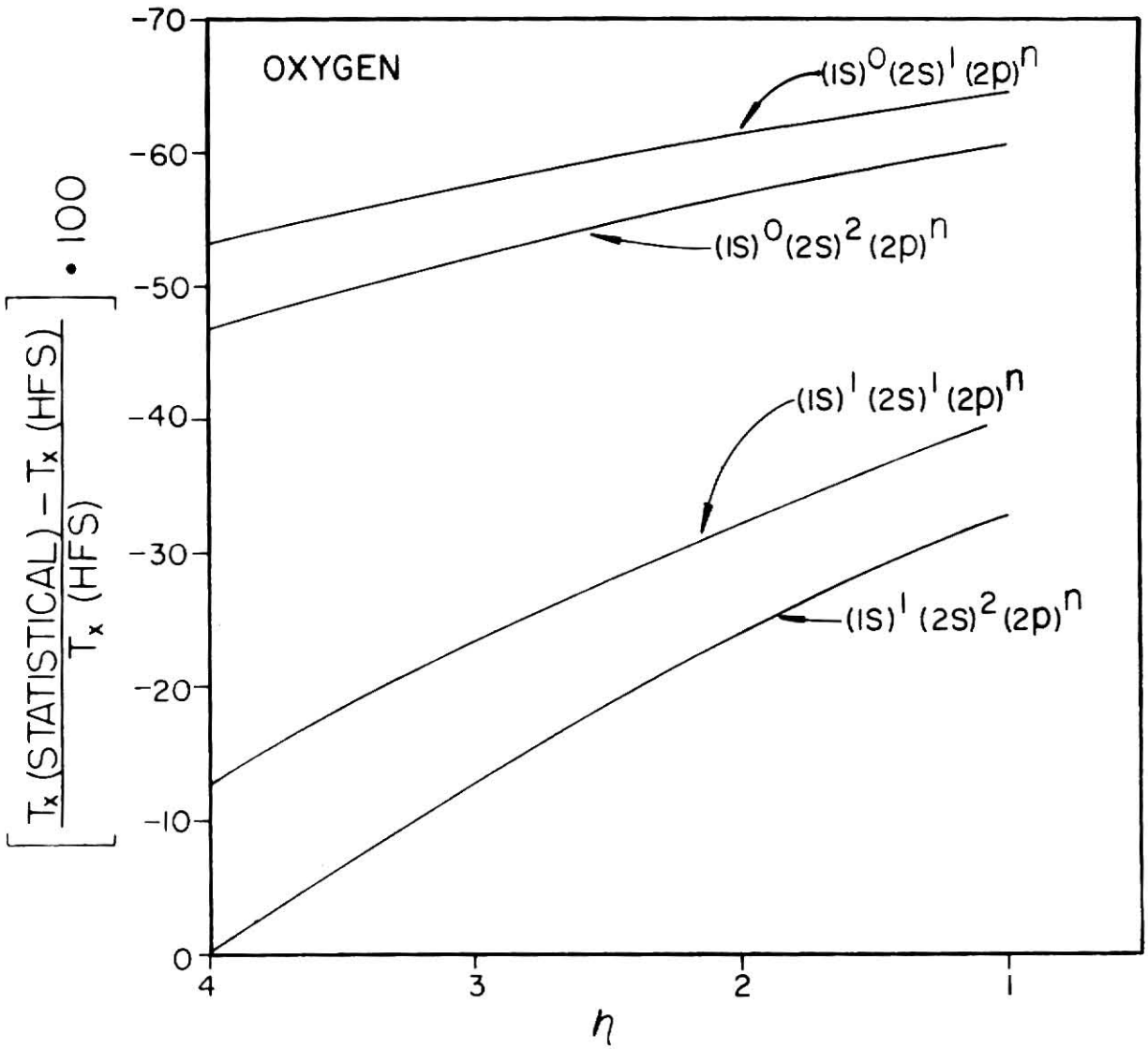

Fig. 6 Percent deviation between the K_α x-ray rates, calculated with the HFS model, and the K_α x-ray rates, calculated with statistical model, versus the number of 2p-shell electrons for various configurations of oxygen.

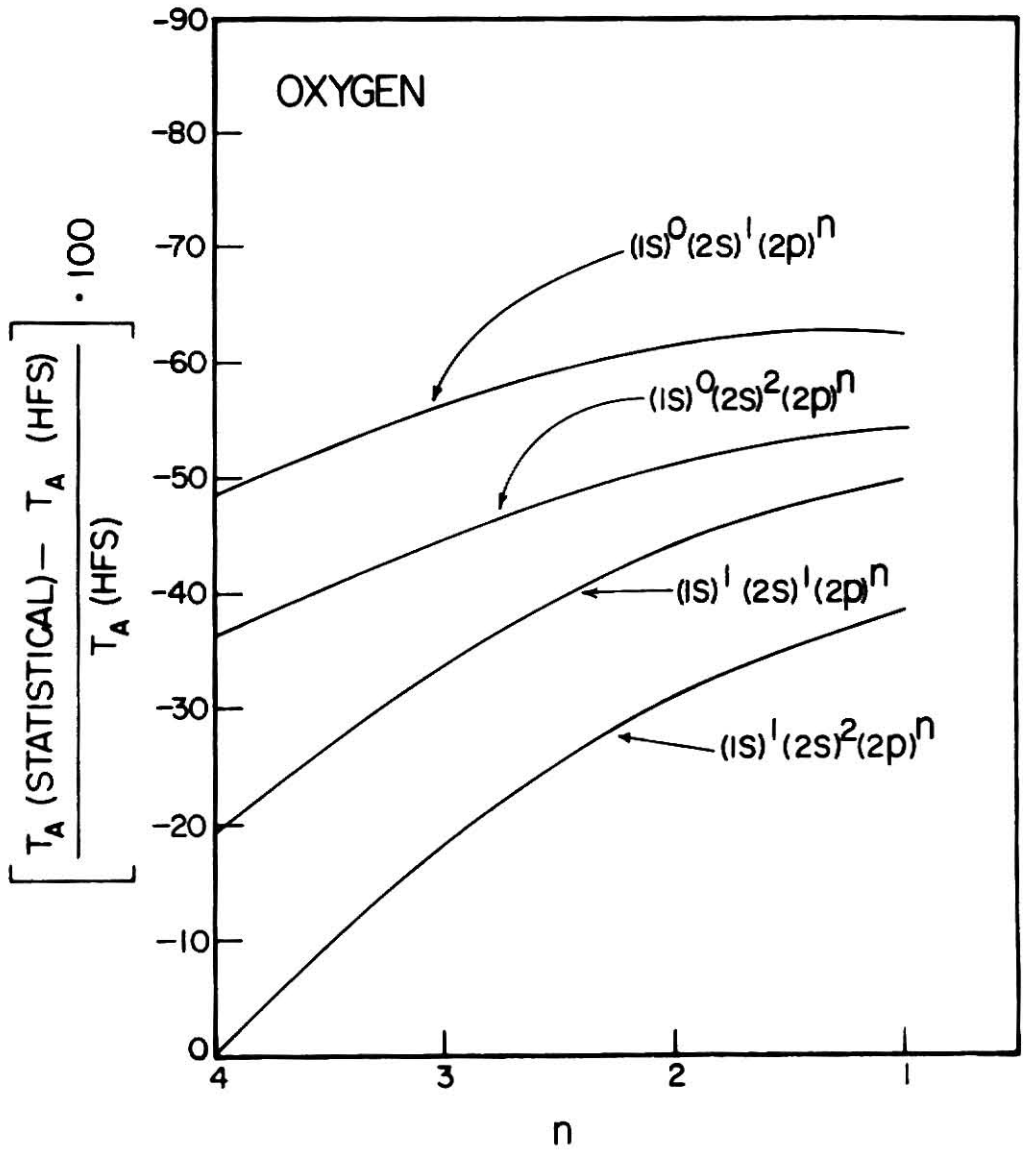

Fig. 7 Percent deviation between the total Auger rates, calculated with the HFS model, and the total Auger rates, calculated with the statistical model, versus the number of 2p-shell electrons for various configurations of oxygen.

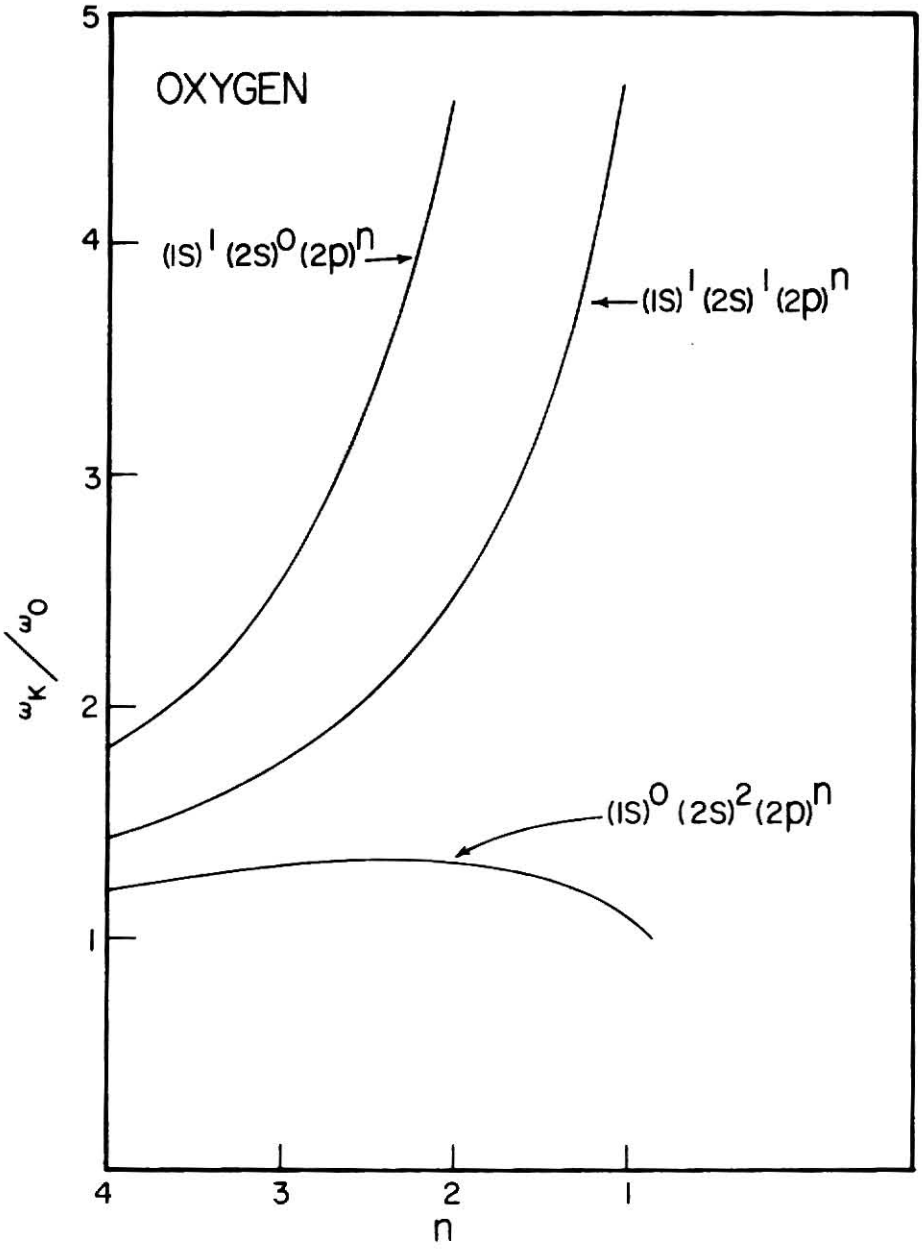

Fig. 8 Normalized K-shell fluorescence yields, calculated with the HFS model, versus the number of 2p-shell electrons for various configurations of oxygen. ω_o is the value of ω_K for the configuration $(1s)^1(2s)^2(2p)^4$.

CHAPTER V

COMPARISON WITH EXPERIMENT

The experimental value[47] of the K-shell fluorescence yield for the electronic configuration $(1s)^1(2s)^2(2p)^6$ is 0.018 ± 0.04, which is to be compared with our calculated value of 0.016. The calculated Auger electron energies are also in excellent agreement with the high-energy resolution measurements[48]. The experimental Auger intensities relative to the 1s-2s-2s (^1S_o) Auger transition for low Z values do not agree with the values calculated in the L-S coupling scheme. The configuration interaction between the final states (^1S_o) arising from the 1s-2s-2s and the 1s-2p-2p Auger transitions has been shown by Asaad[49], and Mehlorn and Asaad[50] to be important. The detailed calculations of Bhalla[51], with the inclusion of the above-mentioned configuration interaction agree reasonably well with the high-energy resolution data of the relative Auger intensities[46]. It should be noted that the total Auger rates are independent of the choice of the coupling scheme.

As mentioned earlier, the K-shell vacancy produced in heavy ion-atom collision is usually accompanied by multiple inner shell ionization. This is in contrast to the proton-atom or electron-atom collisions. Burch et al.[29] have measured the ratios of the yields for the 30 MeV oxygen-neon and the 5 Mev proton-neon collisons. A relative fluorescence yield, ω_K (oxygen)/ω_K (proton) = 2.4 ± 0.5 was obtained. Their measurements also included the x-ray transition energies (2p→1s) and the Auger electron energies. The population of the various defect

configurations of neon, produced in the oxygen-neon collision cannot be inferred by a comparison of the theoretical energy shifts with the low-resolution experimental data.[52] However, the following configurations: $(1s)^1(2s)^1(2p)^3$, $(1s)^1(2s)^1(2p)^2$, $(1s)^1(2s)^0(2p)^4$, and $(1s)^1(2s)^0(2p)^3$ are consistent with the relative fluorescence yield and the observed shifts in the x-ray and Auger transition energies.

CHAPTER VI

DISCUSSION AND CONCLUSIONS

We have presented in this thesis the x-ray rates, the Auger groups rates and the K-shell fluorescence yield for multiply ionized configurations of neon, oxygen and nitrogen. The calculations are performed with the nonrelativistic Hartree-Fock-Slater model and the exchange contributions are included by the HVDO approximation. The shifts in the x-ray transition energies and Auger electron energies are also presented.

The electronic configurations, which are consistent with ΔE_x, ΔE_A and the relative K-shell fluorescence yield in the 30 MeV oxygen-neon collision, were found to be $(1s)^1(2s)^1(2p)^3$, $(1s)^1(2s)^1(2p)^2$, $(1s)^1(2s)^0(2p)^4$, and $(1s)^1(2s)^0(2p)^3$. The relative population of the defect configuration cannot be ascertained until high energy resolution data become available.

The statistical scaling procedure, which is in common use, is found to be in error for most defect configurations of neon, oxygen and nitrogen. This approximate procedure, therefore, should be used with caution for low Z.

In conclusion, the theoretical results for defect configurations of neon, oxygen and nitrogen are presented, and these are essential in the correct interpretation of the experimental data pertaining to heavy ion-gas collisions.

REFERENCES

1. E. J. McGuire, Phys. Rev. 185, 1 (1969); Phys. Rev. A2, 273 (1970); Phys. Rev. A3, 587 (1971); Phys. Rev. A5, 1043 (1972); Phys. Rev. A5, 1052 (1972).
2. D. L. Walters and C. P. Bhalla, Phys. Rev. A3, 519 (1971); Phys. Rev. A3, 1919 (1971); ATOMIC DATA 3, 301 (1971); Phys. Rev. A4, 2164 (1971).
3. C. P. Bhalla, Phys. Rev. A 6, 1409, 1972; in Inner Shell Ionization Phenomena, (North-Holland Pub. Co., 1972) (in press).
4. R. A. Rubenstein, Ph.D. thesis, University of Illinois (1955) performed the first such calculations.
5. G. Wentzel, Z. Physik 43, 524 (1927); L. Pincherle, Nuovo Cimento 12, 81 (1935).
6. E. H. S. Burhop, Proc. Roy. Soc. (London) A148, 272 (1935).
7. E. J. Callan, Phys. Rev. 124, 793 (1961), Rev. Mod. Phys. 35, 524 (1963).
8. V. O. Kostroun, M. H. Chen and B. Crasemann, Phys. Rev. A3, 533 (1971); Phys. Rev. A4, 1 (1971). Chen et al. Phys. Rev. A4, 1 (1971); B. Crasemann, M. H. Chen, V. L. Kostroun, Phys. Rev. A4, 2161 (1971).
9. W. N. Asaad, Proc. Roy. Soc. 249, 555 (1959).
10. M. A. Listengarten, Bull. Akad. Science USSR, Phys. Ser. Vol. 25, 803 (1961); Vol. 24, 182 (1962).
11. C. P. Bhalla and D. J. Ramsdale, Z. Physik 239, 95 (1970); J. Phys. B 3, L14 (1970).

12. C. P. Bhalla, H. R. Rosner and D. J. Ramsdale, J. Phys. B 3, 1232 (1970); Phys. Letters 31A, 212 (1970).

13. C. P. Bhalla, Phys. Rev. A2, 722 (1970).

14. J. H. Scofield, Phys. Rev. 179, 9 (1969).

15. H. R. Rosner and C. P. Bhalla, Z. Physik 231, 347 (1970).

16. C. P. Bhalla, J. Phys. B 3, 916 (1970).

17. For an excellent review, which contains all references up to April 1972, See Hanz-Dieter Betz, Rev. Mod. Phys., 44, 465 (1972).

18. Hans J. Specht, Z. Physik 185, 301 (1965).

19. P. Richard, I. L. Morgan, T. Furuta, and D. Burch, Phys. Rev. Lett. 23, 1009 (1969); D. Burch, and P. Richard, Phys. Rev. Lett. 25, 983 (1970); D. Burch, P. Richard, and R. L. Blake, Phys. Rev. Lett. 26, 100 (1971) D. G. McCray and P. Richard, Phys. Rev. A5, 1249 (1972).

20. A. R. Knudson, D. J. Nagel, P. G. Burkhalter, and K. L. Dunning, Phys. Rev. Lett. 26, 1149 (1971).

21. M. E. Cunningham, R. C. Der, R. J. Fortner, T. M. Kavanagh, J. M. Khan, C. B. Layne, E. J. Zaharis, and J. D. Garcia, Phys. Rev. Lett. 24, 931 (1970).

22. P. H. Mokler, Phys. Rev. Lett. 26, 811 (1971).

23. R. L. Watson and T. K. Li, Phys. Rev. A4, 132 (1971).

24. S. Datz, C. D. Moak, B. R. Appleton, and T. A. Carlson, Phys. Rev. Lett. 27, 363 (1971).

25. J. A. Bearden and A. F. Burr, Rev. Mod. Phys. 39, 125 (1967).

26. M. E. Rudd, T. Jorgensen, D. J. Voltz, Phys. Rev. 151, 28 (1966).

27. P. Richard, W. Hodge and C. Fred Moore, Phys. Rev. Lett. 29, 393 (1972).

28. R. K. Cacak, Q. C. Kessel and M. E. Rudd, Phys. Rev. A2, 1327 (1970) reported $\sigma_A(K)$ for $Ne^+ \rightarrow Ne$, and $\sigma_A(L)$ for $Ar^+ \rightarrow Ar$ in the range of bombarding energies of 50 KeV - 100 KeV. Recently G. N. Ogurtsov, Electronic and Atomic Collisions, VII ICPEAC, Abstracts (1972) page 400, have extended the measurements of $\sigma_A(L)$ for $Ar^+ \rightarrow Ar$ up to 2.5 KeV. The $\sigma_x(K)$ and $\sigma_x(L)$ for these cases were measured by F. W. Saris and D. Onderlinden, Physica 49, 441 (1970). Also see, F. W. Saris, Physics of Electronic and Atomic Collisions, VII ICPEAC (North-Holland Publ. Co.) 1972, page 181, and M. E. Rudd, page 107.

29. D. Burch, W. B. Ingalls, J. S. Risley and R. H. Heffner, Phys. Rev. Lett. 29, 1719 (1972). The authors report $\omega_K/\omega_o = 2.4 \pm 0.5$ where ω_K and ω_o are the K-shell fluorescence yield of neon for the 30 MeV oxygen-neon collision and for the 5 MeV porton-neon collision respectively.

30. Walter Bambynek, Bernd Crasemann R. W. Fink, H. U. Freund, Hans Mark, C. D. Swift, R. E. Price and P. V. Rao, Rev. Mod. Phys. 44, 716 (1972).

31. F. W. Saris, Characteristic X-Ray Production in Heavy Ion-Atom Collisions, Physics of Electronic and Atomic Collisions, VII ICPEAC (North-Holland Publ. Co.) page 181, 1972 has listed all references as of 1971. The invited talks of Patrick Richard, Werner Brandt, T. M. Kavanagh and D. J. Nagel at the International

Conference on Inner-Shell Ionization Phenomena, Atlanta, April 1972 contain all recent references. The Proceedings of this Conference is being published by North-Holland Publishing Company. Also see an extensive review article on the subject by J. D. Garcia, R. J. Fortner and T. M. Kavanagh, Rev. Mod. Phys. April issue (1973).

32. M. Gryzinski, Phys. Rev. 138, A336 (1965).

33. E. Merzbacher and J. S. Khandelwal, Phys. Rev. 151, 12 (1966); J. S. Khandelwal and E. Merzbacher, Phys. Rev. 144, 349 (1966); B. H. Choi and E. Merzbacher, Phys. Rev. 177, 233 (1969); G. S. Khandelwal, B. H. Choi and E. Merzbacher, Atomic Data 1, 103 (1969); Also see Proceedings of the International Conference on Inner-shell Phenomena, North-Holland Pub. Co. 1972 (invited talk by E. Merzbacher).

34. J. D. Garcia, E. Gerjuoy and J. E. Welker, Phys. Rev. 165, 66 (1968); J. D. Garcia, Phys. Rev. 159, 39 (1967); B. K. Thomas and J. D. Garcia, Phys. Rev. 179, 94 (1969); J. D. Garcia, Phys. Rev. 177, 223 (1969); J. D. Garcia, Phys. Rev. A1, 280 (1970).

35. For the low incident ion velocities, the mechanism of creating the inner shell vacancy is better described by the electron promotion mechanism of W. Lichten and U. Fano, Phys. Rev. Lett. 14, 627 (1965). W. Lichten, Phys. Rev. 164, 131 (1967); M. Barat and W. Lichten, Phys. Rev. 6, 211 (1972); The explicit calculations have been performed by J. S. Briggs and J. Macek, J. Phys. B 5, 579 (1972),

and also by F. P. Larkins, Proceedings of the Inner Shell Ionization Phenomena (North-Holland Pub. Co.) 1972.

36. The Landau-Zener theory of level crossing has been successfully utilized for parameterization of the K-shell cross sections. See for example, R. C. Der, R. J. Fortner, T. M. Kavangh and J. M. Khan, Phys. Rev. 4, 556 (1971).

37. F. P. Larkins, J. Phys. B4, L29 (1971).

38. R. J. Fortner, R. C. Der, T. M. Kavanagh and J. D. Garcia, J. Phys. B5, L73 (1972).

39. C. P. Bhalla and D. L. Walters in Inner Shell Ionization Phenomena (North-Holland Publ. Co., 1972)(in press).

40. F. Herman and K. Schwarz, in Computational Solid State Physics (Plenum Press, New York 1972).

41. F. Herman and S. Skillman, Atomic Structure Calculations (Prentice Hall, Inc., Englewood Cliffs, N.J. 1963).

42. J. C. Slater, Quantum Theory of Atomic Structure, Vol. I, II, (McGraw-Hill Book Company, New York 1960).

43. B. W. Shore and D. H. Menzel, Principles of Atomic Spectra (John Wiley and Sons, Inc., New York 1968).

44. H. Korber and W. Mehlhorn, Zeit. Physik 191, 217 (1966); M. O. Krause, T. A. Carlson and W. E. Moddeman, J. Physics (Paris) Colloq. C4, 139 (1971).

45. Volker Schmidt, in Inner Shell Ionization Phenomena (North-Holland Publishing Company) (in press).

46. M. O. Krause, F. A. Stevie, L. J. Lewis, T. A. Carlson and W. E. Moddeman, Phys. Letters 31A, 81 (1970).

47. J. Heinz, Z. Physik 143, 153 (1955).

48. Kai Siegbahn et al. ESCA, Uppsala 1967, page 158.

49. W. N. Asaad, Nuclear Physics 66, 494 (1965).

50. W. Mehlhorn and W. N. Asaad, Z. Physik 191, 231 (1966).

51. C. P. Bhalla, to be submitted for publication.

52. C. P. Bhalla and M. Hein, Phys. Rev. Letters 30, 39 (1973).

APPENDIX A

CALCULATION OF TOTAL ENERGY

A numerical subroutine was employed to calculate the total energy and its constituent parts for the atomic systems investigated in this thesis. The results of these calculations are presented in Tables I through XI. To obtain the total energy of an atomic system one can calculate the expectation value of the HF Hamiltonian, using the HF bound state wave-functions.

The HF Hamiltonian is,

$$H = \sum_i \left(\frac{p_i^2}{2m} - \frac{Z e^2}{r_i} \right) + \tfrac{1}{2} \sum_{i \neq j} \frac{e^2}{r_{ij}} \quad . \tag{1}$$

The total energy is then given by,

$$E_{HF} = \langle \psi_{HF} | H | \psi_{HF} \rangle$$

$$E_{HF} = \sum_i \langle \phi_i | \frac{p_i^2}{2m} | \phi_i \rangle - \sum_i \langle \phi_i | \frac{Z e^2}{r_i} | \phi_i \rangle$$

$$+ \tfrac{1}{2} \sum_{i,j} \langle \phi_i(1) \phi_j(2) | \frac{e^2}{r_{12}} | \phi_i(1) \phi_j(2) \rangle$$

$$- \tfrac{1}{2} \sum_{i,j} \langle \phi_i(1) \phi_j(2) | \frac{e^2}{r_{12}} | \phi_i(2) \phi_j(1) \rangle \quad .$$

or,

$$E_{HF} = KE + NIE + DEIE + XEIE \quad , \tag{2}$$

where KE is the kinetic energy, NIE is the Coulomb nuclear interaction energy, DEIE is the direct electron-electron interaction energy, and XEIE is the exchange electron-electron interaction energy.

To scale to atomic units we take $\frac{\hbar^2}{2m a_0^2} = \frac{e^2}{2 a_0} \equiv 1\, Ry$.

For further convenience take $\phi_i(\vec{r}) = R_{n\ell}(r)\, Y_{\ell m}(\hat{r})\, \alpha_\sigma$,

and define $P_{n\ell}(r) \equiv r R_{n\ell}(r)$, where the $R_{n\ell}(r)$ are the radial

functions, $Y_{\ell m}(\hat{r})$ are the angular functions, and α_σ are the spin functions.

Consider the terms of equation (2) separately:

KE ≡

$$\langle \phi_i | \frac{p^2}{2m} | \phi_i \rangle = 1\,R_y \langle R_{n\ell}(r) Y_{\ell m}(\hat{r}) | -\nabla^2 | R_{n\ell}(r) Y_{\ell m}(\hat{r}) \rangle$$
$$= 1\,R_y \int_0^\infty \left\{ \left(\frac{d}{dr} P_{n\ell} \right)^2 + \frac{\ell(\ell+1)}{r^2} P_{n\ell}^2 \right\} dr \ .$$

NIE ≡

$$\langle \phi_i | -\frac{Ze^2}{r} | \phi_i \rangle = -2\,Z\,R_y \int_0^\infty \frac{P_{n\ell}^2}{r}\, dr \ .$$

DEIE ≡

$$\sum_{i,j} \langle \phi_i(1)\phi_j(2) | \frac{e^2}{r_{12}} | \phi_i(1)\phi_j(2) \rangle =$$

$$2\,R_y \sum_{n\ell m\sigma} \sum_{n'\ell' m'\sigma'} \int d^3r_1\, R_{n\ell}(r_1) |Y_{\ell m}(\hat{r}_1)|^2 \int d^3r_2\, R_{n'\ell'}(r_2) |Y_{\ell' m'}(\hat{r}_2)|^2 \frac{1}{|\vec{r}_1 - \vec{r}_2|} \ .$$

For closed shells $4\pi \sum_{m\sigma} |Y_{\ell m}(\hat{r})|^2 = 2(2\ell+1)$.

To account for non-closed shell, we take $4\pi \sum_{m\sigma} |Y_{\ell m}(\hat{r})|^2 = N(n,\ell)$.

Expanding $\frac{1}{|\vec{r}_1 - \vec{r}_2|} = \sum_k \frac{r_<^k}{r_>^{k+1}} P_k(\hat{r}_1 \cdot \hat{r}_2)$, and performing the anuglar intergration, only the $K=0$ term contributes, so we get

$$DEIE = 1\,R_y \sum_{n,\ell} N(n,\ell) \sum_{n',\ell'} N'(n',\ell') \int_0^\infty P_{n\ell}^2(r_1)\, dr_1 \int_0^\infty P_{n'\ell'}(r_2)\, dr_2 \frac{1}{r_>} \ .$$

XEIE ≡

$$\sum_{i,j} \langle \phi_i(1)\phi_j(2) | \frac{e^2}{r_{12}} | \phi_i(2)\phi_j(1) \rangle =$$

$$2\,R_y \sum_{n,\ell m\sigma} \sum_{n'\ell' m'\sigma'} \int d^3r_1\, R_{n\ell}(r_1)\, Y^*_{\ell m}(\hat{r}_1)\, R_{n'\ell'}(r_1)\, Y_{\ell' m'}(\hat{r}_1)\, \alpha^*_{\sigma'} \cdot \alpha_{\sigma'} \times$$

$$\int d^3r_2\, R_{n'\ell'}(r_2)\, Y^*_{\ell' m'}(\hat{r}_2)\, R_{n\ell}(r_2)\, Y_{\ell m}(\hat{r}_2)\, \alpha^*_{\sigma'} \cdot \alpha_\sigma \frac{1}{|\vec{r}_1 - \vec{r}_2|} \ .$$

Making the assumption that the spins are paired, the integral over the cross terms cancel, and the integral over the direct terms contribute a factor of 2, so,

$$XEIE = 2R_y \times 2 \sum_{n,\ell} \sum_{n'\ell'} \int_0^\infty r_1^2 dr_1 R_{n\ell}(r_1) R_{n'\ell'}(r_1) \int_0^\infty r_2^2 dr_2 R_{n\ell}(r_2) R_{n'\ell'}(r_2) \times$$

$$\iint d\Omega_1 d\Omega_2 \sum_m \sum_{m'} \sum_{\kappa m''} \frac{4\pi}{(2\kappa+1)} \frac{r_<^\kappa}{r_>^{\kappa+1}} Y^*_{\ell m}(\hat{r}_1) Y_{\ell' m'}(\hat{r}_1) Y_{\kappa m''}(\hat{r}_1) Y_{\ell m}(\hat{r}_2) Y^*_{\ell' m'}(\hat{r}_2) Y^*_{\kappa m''}(\hat{r}_2)$$

Now express the three sums over azimuthal indecies of the product spherical harmonics as Legendre functions.

Note that we have already taken into account the spin so the factor corresponding to $\frac{(2\ell+1)}{4\pi}$ is $\frac{N(n,\ell)}{2}$. Performing the above operations we get,

$$XEIE = -\tfrac{1}{2} R_y \sum_{n,\ell} N(n,\ell) \sum_{n'\ell'} N'(n';\ell') \int_0^\infty dr_1 P_{n\ell}(r_1) P_{n'\ell'}(r_1) \times$$

$$\int_0^\infty dr_2 P_{n\ell}(r_2) P_{n'\ell'}(r_2) \sum_\kappa \frac{r_<^\kappa}{r_>^{\kappa+1}} \iint d\Omega_1 d\Omega_2 P_\ell(\hat{r}_1 \cdot \hat{r}_2) P_{\ell'}(\hat{r}_1 \cdot \hat{r}_2) P_\kappa(\hat{r}_1 \cdot \hat{r}_2)/(4\pi)^2$$

or,

$$XEIE = -\tfrac{1}{2} R_y \sum_{n,\ell} N(n,\ell) \sum_{n'\ell'} N'(n';\ell') \int_0^\infty dr_1 P_{n\ell}(r_1) P_{n'\ell'}(r_1) \int_0^\infty dr_2 P_{n\ell}(r_2) P_{n'\ell'}(r_2) \times f(\ell,\ell';r,r') \ .$$

$$f(\ell,\ell';r,r') \equiv \sum_\kappa \frac{r_<^\kappa}{r_>^{\kappa+1}} A_\kappa(\ell,\ell') \quad ;$$

$$A_\kappa(\ell,\ell') \equiv \iint d\Omega_1 d\Omega_2 P_\ell(\hat{r}_1 \cdot \hat{r}_2) P_{\ell'}(\hat{r}_1 \cdot \hat{r}_2) P_\kappa(\hat{r}_1 \cdot \hat{r}_2)/(4\pi)^2 \ .$$

Further,

$$A_\kappa(\ell,\ell') = \tfrac{1}{2} \int_{-1}^{1} dx \, P_\ell(x) P_{\ell'}(x) P_\kappa(x)$$

or in terms of $3j$ symbols[1],

$$A_\kappa(\ell,\ell') = \begin{pmatrix} \ell & \ell' & \kappa \\ 0 & 0 & 0 \end{pmatrix}^2 \ .$$

The total energy is found by summing up the four separate parts, as in equation (2).

By specializing the notation to that employed previously, and restricting the shells to those up to and including the 2p-shell, we can simplify the total energy expression.

As before, we define

$$R^{\kappa}(1,2,3,4) \equiv \int_0^{\infty}\int_0^{\infty} P_{n_1\ell_1}(r_i) P_{n_2\ell_2}(r_j) \frac{r_<^{\kappa}}{r_>^{\kappa+1}} P_{n_3\ell_3}(r_i) P_{E\ell_4}(r_i)\, dr_i\, dr_j \quad .$$

Then,

$$DEIE = \tfrac{1}{2} \sum_{n,\ell} N(n,\ell) \sum_{n',\ell'} N'(n',\ell')\, R^0(n\ell, n'\ell', n\ell, n'\ell') \quad ;$$

$$XEIE = -\tfrac{1}{4} \sum_{n,\ell} N(n,\ell) \sum_{n',\ell'} N'(n',\ell') \sum_{\kappa} R^{\kappa}(n\ell, n\ell, n'\ell', n'\ell')\, A_{\kappa}(\ell,\ell')$$

where $A_{\kappa} = \begin{pmatrix} \ell & \ell' & \kappa \\ 0 & 0 & 0 \end{pmatrix}^2$.

In general $N(n,\ell)\,N'(n',\ell')$ is the product of the full-shell occupation numbers, multiplied by the existing number of possible pairs of electrons, and divided by the full-shell number of pairs of electrons. This procedure guarantees that each term is averaged correctly. Let m_1 and n_1 be the actual occupation numbers and m_0 and n_0 be the full-shell occupation numbers of two distinct shells. Then

$$N(n,\ell)\,N'(n',\ell') = \begin{cases} m_1 n_1 & n' \neq n \text{ and } \ell' \neq \ell \\ \dfrac{n_1(n_1-1)\,n_0^2}{n_0(n_0-1)} & n' = n \text{ and } \ell' = \ell \end{cases} \quad .$$

So for the general configuration $(1s)^{\ell}(2s)^{m}(2p)^{n}$,

we obtain,

$$\begin{aligned} DEIE = \tfrac{1}{2}\big[& 2\ell(\ell-1)R^0(1s,1s,1s,1s) + 2m(m-1)R^0(2s,2s,2s,2s) \\ & + \tfrac{6}{5} n(n-1) R^0(2p,2p,2p,2p) + 2\ell m R^0(1s,2s,1s,2s) \\ & + 2\ell n R^0(1s,2p,1s,2p) + 2mn R^0(2s,2p,2s,2p)\big] \end{aligned}$$

and,

$$\text{XEIE} = -\tfrac{1}{4}\{2\ell(\ell-1)R^0(1s,1s,1s,1s) + 2m(m-1)R^0(2s,2s,2s,2s)$$
$$+ \tfrac{6}{5}n(n-1)[\tfrac{1}{3}R^0(2p,2p,2p,2p) + \tfrac{2}{15}R^2(2p,2p,2p,2p)]$$
$$+ 2\ell m R^0(1s,1s,2s,2s) + \tfrac{2}{3}\ell n R^1(1s,1s,2p,2p)$$
$$+ \tfrac{2}{3}mn R^1(2s,2s,2p,2p)\} \;;$$

$$E_{HF} = KE + NIE + DEIE + XEIE \quad .$$

This total energy is consistent with the results given by Slater [2]. In Slater's notation $F^0(n\ell, n'\ell') \equiv R^0(n\ell, n'\ell', n\ell, n'\ell') = F^0(n'\ell', n\ell)$ and $G^\kappa(n\ell, n'\ell') \equiv R^\kappa(n\ell, n\ell, n'\ell', n'\ell') = G^\kappa(n'\ell', n\ell)$, and the total energy in Rydbergs is given by,

$$E_{HF} = KE + NIE + \frac{\ell(\ell-1)}{2}F^0(1s,1s) + \frac{m(m-1)}{2}F^0(2s,2s)$$
$$+ \frac{n(n-1)}{2}[F^0(2p,2p) - \tfrac{2}{25}F^2(2p,2p)] + \ell m[F^0(1s,2s) - \tfrac{1}{2}G^0(1s,2s)]$$
$$+ \ell n[F^0(1s,2p) - \tfrac{1}{6}G^1(1s,2p)] + mn[F^0(2s,2p) - \tfrac{1}{6}G^1(2s,2p)] \quad .$$

An analogous treatment can be made to obtain the HF binding energy, ϵ_j .

$$H\phi(1) = \left(\frac{p_1^2}{2m} - \frac{Ze^2}{r_1}\right)\phi(1) + \sum_i \int d^3r_2\, \phi_i^*(2)\frac{e^2}{|\vec{r}_1 - \vec{r}_2|}\left(\phi_i(2)\phi(1) - \phi_i(1)\phi(2)\right) \quad .$$

$$\epsilon_j = \int d^3r_1\, \phi_j^*(1) H \phi_j(1) = KE_j + E_{dj} + E_{xj} \;,$$

where KE_j , E_{d_j} , and E_{x_j} are the kinetic, direct electron-electron, and exchange electron-electron contributions respectively. j now denotes the set of quantum lables of the jth. electron.

$$KE_j = 1R_y \int_0^\infty dr \left\{ \left(\frac{d}{dr} P_j\right)^2 + \frac{\ell(\ell+1)}{r^2} P_j^2 \right\} .$$

$$E_{d_j} = 1R_y \int_0^\infty dr_1 P_j(r_1) V_d(r_1)$$

where $$V_d(r_1) \equiv -\frac{2Z}{r_1} + 2\int_0^\infty dr_2 \frac{Q(r_2)}{r_>}$$

and $$Q(r) \equiv \sum_{n,\ell} N(n,\ell) P_{n\ell}^2 .$$

$$E_{x_j} = -1R_y \sum_{n,\ell} \frac{N(n,\ell)}{2} \int_0^\infty dr_1 P_j(r_1) P_{n\ell}(r_1) \int_0^\infty dr_2 P_j(r_2) P_{n\ell}(r_2) f(\ell,\ell_j,r,r') ,$$

where $$f(\ell,\ell_j,r,r') \equiv \sum_k \frac{r_<^k}{r_>^{k+1}} A_k(\ell,\ell_j)$$

and

$$A_k(\ell,\ell_j) \equiv \iint d\Omega_j d\Omega_2 \, P_\ell(\hat{r}_j\cdot\hat{r}_2) P_{\ell_j}(\hat{r}_j\cdot\hat{r}_2) P_k(\hat{r}_j\cdot\hat{r}_2)/(4\pi)^2 .$$

REFERENCES

1. A. R. Edmonds, Angular Momentum in Quantum Mechanics, (Princeton University Press, Princeton, New Jersey 1957).

2. J. C. Slater, Quantum Theory of Atomic Structure, Vol. I, II, (McGraw-Hill Book Company, New York 1960).

TABLE I Calculated H.F. binding energy, kinetic energy, nuclear interaction energy, electron-electron interaction energy in Rydbergs, and <r> in Angstroms for neon with configuration ($1s^2 2s^2 2p^n$).

Configuration	shell	HF.B.E.	K.E.	N.I.E.	E.E.I.E.	EX.E.	<r> in Å
$1s^2 2s^2 2p^6$	1s	-65.9397	92.6073	-192.4215	46.3094	-12.4348	0.0835
$1s^2 2s^2 2p^6$	2s	-4.0857	10.4977	-32.6484	21.4484	-3.3833	0.4777
$1s^2 2s^2 2p^6$	2p	-1.8972	8.3128	-28.0842	20.5284	-2.6542	0.5440
			Total Energy = -256.9961				
$1s^2 2s^2 2p^5$	1s	-67.5898	92.6328	-192.4486	44.6586	-12.4326	0.0835
$1s^2 2s^2 2p^5$	2s	-5.4087	11.0530	-33.4993	20.3662	-3.3286	0.4634
$1s^2 2s^2 2p^5$	2p	-3.3719	9.3542	-30.1014	20.2225	-2.8472	0.4854
			Total Energy = -255.5582				

TABLE I (cont.)

$1s^2 2s^2 2p^4$	1s	-69.6336	92.6894	-192.5089	42.6119	-12.42589	0.0834
$1s^2 2s^2 2p^4$	2s	-6.9650	11.8228	-34.6290	19.1001	-3.2589	0.4659
$1s^2 2s^2 2p^4$	2p	-5.1089	10.4437	-32.0000	19.4500	-3.0026	0.4444
			Total Energy = -252.5548				
$1s^2 2s^2 2p^3$	1s	-72.0395	92.7854	-192.6107	40.1977	-12.4120	0.0833
$1s^2 2s^2 2p^3$	2s	-8.7194	12.7420	-35.9192	17.6285	-3.1708	0.4297
$1s^2 2s^2 2p^3$	2p	-7.0816	11.5694	-33.8078	18.2858	-3.1291	0.4127
			Total Energy = -247.7413				
$1s^2 2s^2 2p^2$	1s	-74.7868	92.9387	-192.7731	37.4368	-12.3893	0.0833
$1s^2 2s^2 2p^2$	2s	-10.6522	13.7602	-37.2893	15.9397	-3.0629	0.4135
$1s^2 2s^2 2p^2$	2p	-9.2751	12.7166	-35.5296	16.7684	-3.2305	0.3872
			Total Energy = -240.8906				

TABLE I (cont.)

$1s^2 2s^2 2p^1$	1s	-77.8563	93.1711	-193.0185	34.3481	-12.3571	0.0831
$1s^2 2s^2 2p^1$	2s	-12.7502	14.8224	-38.6669	14.0286	-2.9344	0.3986
$1s^2 2s^2 2p^1$	2p	-11.6756	13.8549	-37.1421	14.9188	-3.3073	0.3662
			Total Energy = -231.7796				

TABLE II Calculated H.F. binding energy, kinetic energy, nuclear interaction energy, electron-electron interaction energy in Rydbergs, and <r> in Angstroms for neon with configuration ($1s^2 2s^1 2p^n$).

Configuration	Shell	HF.B.E.	K.E.	N.I.E.	E.E.I.E.	EX.E.	<r> In Å
$1s^2 2s^1 2p^6$	1s	-67.5419	92.6732	-192.4898	44.6541	-12.3795	0.0835
$1s^2 2s^1 2p^6$	2s	-5.6440	11.0448	-33.4899	20.3357	-3.5547	0.4633
$1s^2 2s^1 2p^6$	2p	-3.2528	9.3475	-30.0956	20.2100	-2.7147	0.4851
			Total Energy = -253.4057				
$1s^2 2s^1 2p^5$	1s	-69.5337	92.7218	-192.5415	42.6563	-12.3703	0.0834
$1s^2 2s^1 2p^5$	2s	-7.1835	11.7754	-34.5625	19.0735	-3.4699	0.4474
$1s^2 2s^1 2p^5$	2p	-4.9507	10.3855	-31.9074	19.4259	-2.8548	0.4458
			Total Energy = -250.5203				
$1s^2 2s^1 2p^4$	1s	-71.8802	92.8090	-192.6337	40.2985	-12.3539	0.0834
$1s^2 2s^1 2p^4$	2s	-8.9194	12.6550	-35.7996	17.6130	-3.3877	0.4310
$1s^2 2s^1 2p^4$	2p	-6.8825	11.4708	-33.6575	18.2750	-2.9708	0.4149
			Total Energy = -245.8754				

TABLE II (cont.)

$1s^2 2s^1 2p^3$	1s	-74.5646	92.9432	-192.7760	37.5969	-12.3286	0.0833
$1s^2 2s^1 2p^3$	2s	-10.8333	13.6384	-37.1274	15.9427	-3.2871	0.4153
$1s^2 2s^1 2p^3$	2p	-9.0339	12.5890	-35.3448	16.7873	-3.0654	0.3895
			Total Energy = -239.2430				
$1s^2 2s^1 2p^2$	1s	-77.5694	93.1415	-192.9855	34.5678	-12.2933	0.0831
$1s^2 2s^1 2p^2$	2s	-12.9130	14.6866	-38.4914	14.0593	-3.1675	0.4004
$1s^2 2s^1 2p^2$	2p	-11.3932	13.7174	-36.9527	14.9811	-3.1390	0.3684
			Total Energy = -230.4007				
$1s^2 2s^1 2p^1$	1s	-80.8683	93.4176	-193.2761	31.2385	-12.2482	0.0829
$1s^2 2s^1 2p^1$	2s	-15.1475	15.8029	-39.8995	11.9792	-3.0341	0.3859
$1s^2 2s^1 2p^1$	2p	-13.9468	14.8343	-38.4676	12.8802	-3.1937	0.3503
			Total Energy = -219.1369				

TABLE III Calculated H.F. binding energy, kinetic energy, nuclear interaction energy, electron-electron interaction energy in Rydbergs and <r> in Angstroms for neon with configuration ($1s^2 2s^0 2p^n$).

Configuration	Shell	HF.B.E.	K.E.	N.I.E.	E.E.I.E.	EX.E.	<r> In Å
$1s^2 2s^0 2p^6$	1s	-69.4407	92.7637	-192.5841	42.6950	-12.3154	0.0834
$1s^2 2s^0 2p^6$	2p	-4.7962	10.3274	-31.8150	19.3990	-2.7076	0.4472
			Total Energy = -248.1124				
$1s^2 2s^0 2p^5$	1s	-71.7318	92.8398	-192.6648	40.3898	-12.2966	0.0834
$1s^2 2s^0 2p^5$	2p	-6.6886	11.3716	-33.5058	18.2587	-2.8131	0.4170
			Total Energy = -243.6140				
$1s^2 2s^0 2p^4$	1s	-74.3549	92.9613	-192.7932	37.7461	-12.2690	0.0833
$1s^2 2s^0 2p^4$	2p	-8.7991	12.4562	-35.1520	16.7970	-2.9004	0.3920
			Total Energy = -237.1766				
$1s^2 2s^0 2p^3$	1s	-77.2961	93.1352	-192.9770	34.7769	-12.2313	0.0832
$1s^2 2s^0 2p^3$	2p	-11.1172	13.5638	-36.7410	15.0299	-2.9699	0.3707
			Total Energy = -228.5795				

TABLE III (cont.)

$1s^2 2s^0 2p^2$	1s	-80.5249	93.3636	-193.2174	31.5111	-12.1822	0.0830
$1s^2 2s^0 2p^2$	2p	-13.6322	14.7253	-38.3267	12.9993	-3.0302	0.3515
			Total Energy = -217.6122				
$1s^2 2s^0 2p^1$	1s	-83.9658	93.0471	-192.8838	27.9484	-12.0775	0.0832
$1s^2 2s^0 2p^1$	2p	-16.3748	16.8172	-40.9984	10.9874	-3.1810	0.3246
			Total Energy = -204.0805				

TABLE IV Calculated H.F. binding energy, kinetic energy, nuclear interaction energy, electron-electron interaction energy in Rydbergs, and <r> in Angstroms for neon with configuration ($1s^1 2s^2 2p^n$).

Configuration	Shell	HF.B.E.	K.E.	N.I.E.	E.E.I.E.	EX.E.	<r> In Å
$1s^1 2s^2 2p^6$	1s	-74.6642	97.2625	-197.2262	38.2249	-12.9254	0.0811
$1s^1 2s^2 2p^6$	2s	-5.8420	12.4245	-35.4453	20.8018	-3.6230	0.4403
$1s^1 2s^2 2p^6$	2p	-3.7800	11.4577	-33.3481	21.2814	-3.1711	0.4373
			Total Energy = -193.1879				
$1s^1 2s^2 2p^5$	1s	-76.8497	97.3346	-197.3000	36.0331	-12.9175	0.0810
$1s^1 2s^2 2p^5$	2s	-7.4961	13.3088	-36.6742	19.4166	-3.5474	0.4240
$1s^1 2s^2 2p^5$	2p	-5.6419	12.6272	-35.2005	20.2458	-3.3144	0.4040
			Total Energy = -189.8071				
$1s^1 2s^2 2p^4$	1s	-79.3952	97.4539	-197.4220	33.4745	-12.9017	0.0810
$1s^1 2s^2 2p^4$	2s	-9.3446	14.3451	-38.0499	17.8122	-3.4520	0.4079
$1s^1 2s^2 2p^4$	2p	-7.7404	13.8358	-36.9762	18.8298	-3.4298	0.3777
			Total Energy = -184.4926				

TABLE IV (cont.)

$1s^1 2s^2 2p^3$	1s	-82.2818	97.6374	-197.6099	30.5676	-12.8768	0.0808
$1s^1 2s^2 2p^3$	2s	-11.3702	15.4893	-39.5058	15.9828	-3.3365	0.3927
$1s^1 2s^2 2p^3$	2p	-10.0611	15.0720	-38.6819	17.0697	-3.5210	0.3561
			Total Energy = -177.0203				
$1s^1 2s^2 2p^2$	1s	-85.4932	97.9053	-197.8831	27.3264	-12.8418	0.0807
$1s^1 2s^2 2p^2$	2s	-13.5620	16.7004	-40.9888	13.9275	-3.2011	0.3786
$1s^1 2s^2 2p^2$	2p	-12.5928	16.3128	-40.3033	14.9867	-3.5890	0.3381
			Total Energy = -167.1691				
$1s^1 2s^2 2p^1$	1s	-89.0125	98.2924	-198.2764	23.7689	-12.7974	0.0805
$1s^1 2s^2 2p^1$	2s	-15.9102	17.9247	-42.4384	11.6494	-3.0459	0.3657
$1s^1 2s^2 2p^1$	2p	-15.3224	17.5135	-41.8002	12.5967	-3.6324	0.3230
			Total Energy = -154.7267				
$1s^1 2s^2 2p^0$	1s	-92.8122	98.8601	-198.8512	19.9268	-12.7480	0.0801
$1s^1 2s^2 2p^0$	2s	-18.4015	19.0700	-43.7576	9.1561	-2.8700	0.3542
			Total Energy = -139.4907				

TABLE V Calculated H.F. binding energy, kinetic energy, nuclear interaction energy, electron-electron interaction energy in Rydbergs, and <r> in Angstroms for neon with configuration ($1s^1 2s^1 2p^n$).

Configuration	Shell	HF.B.E.	K.E.	N.I.E.	E.E.I.E.	EX.E.	<r> In Å
$1s^1 2s^1 2p^6$	1s	-76.6803	97.2995	-197.2640	36.1429	-12.8587	0.0811
$1s^1 2s^1 2p^6$	2s	-7.7007	13.1961	-36.5250	19.3909	-3.7627	0.4256
$1s^1 2s^1 2p^6$	2p	-5.4422	12.5013	-35.0154	20.2241	-3.1522	0.4065
			Total Energy = -187.7062				
$1s^1 2s^1 2p^5$	1s	-79.1632	97.4007	-197.3673	33.6436	-12.8401	0.0810
$1s^1 2s^1 2p^5$	2s	-9.5304	14.1903	-37.8508	17.8040	-3.6740	0.4099
$1s^1 2s^1 2p^5$	2p	-7.4979	13.6747	-36.7507	18.8378	-3.2598	0.3805
			Total Energy = -182.5951				
$1s^1 2s^1 2p^4$	1s	-81.9839	97.5555	-197.5258	30.7986	-12.8123	0.0809
$1s^1 2s^1 2p^4$	2s	-11.5370	15.2975	-39.2666	15.9982	-3.5660	0.3949
$1s^1 2s^1 2p^4$	2p	-9.7754	14.8874	-38.4353	17.1187	-3.3462	0.3588
			Total Energy = -175.3767				

TABLE V (cont.)

$1s^1 2s^1 2p^3$	1s	-85.1287	97.7769	-197.7520	27.6200	-12.7736	0.0808
$1s^1 2s^1 2p^3$	2s	-13.7097	16.4844	-40.7275	13.9722	-3.4388	0.3809
$1s^1 2s^1 2p^3$	2p	-12.2645	16.1219	-40.0595	15.0856	-3.4124	0.3405
			Total Energy = -165.8315				
$1s^1 2s^1 2p^2$	1s	-88.5829	98.0894	-198.0702	24.1220	-12.7241	0.0806
$1s^1 2s^1 2p^2$	2s	-16.0403	17.7183	-42.1945	11.7296	-3.2937	0.3678
$1s^1 2s^1 2p^2$	2p	-14.9551	17.3490	-41.5987	12.7523	-3.4577	0.3249
			Total Energy = -153.7448				
$1s^1 2s^1 2p^1$	1s	-92.3220	98.5169	-198.5044	20.3310	-12.6656	0.0803
$1s^1 2s^1 2p^1$	2s	-18.5198	18.9989	-43.6688	9.2852	-3.1351	0.3553
$1s^1 2s^1 2p^1$	2p	-17.8322	18.5293	-43.0185	10.1398	-3.4828	0.3115
			Total Energy = -138.9103				
$1s^1 2s^1 2p^0$	1s	-96.2314	98.1198	-198.1024	16.2906	-12.5394	0.0805
$1s^1 2s^1 2p^0$	2s	-21.1418	21.6675	-46.5605	6.7759	-3.0247	0.3377
			Total Energy = -121.1245				

TABLE VI Calculated H.F. binding energy, kinetic energy, nuclear interaction energy, electron-electron interaction energy in Rydbergs, and <r> in Angstroms for neon with configuration ($1s^1 2s^0 2p^n$).

Configuration	Shell	HF.B.E.	K.E.	N.I.E.	E.E.I.E.	EX.E.	<r> In Å
$1s^1 2s^0 2p^6$	1s	-78.9461	97.3599	-197.3256	33.7996	-12.7800	0.0810
$1s^1 2s^0 2p^6$	2p	-7.2635	13.5122	-36.5223	18.8374	-3.0908	0.3833
			Total Energy = -180.2766				
$1s^1 2s^0 2p^5$	1s	-81.7032	97.4927	-197.4615	31.0151	-12.7495	0.0810
$1s^1 2s^0 2p^5$	2p	-9.4985	14.6944	-38.1768	17.1556	-3.1717	0.3617
			Total Energy = -173.2882				
$1s^1 2s^0 2p^4$	1s	-84.7823	97.6833	-197.6563	27.8987	-12.7081	0.0808
$1s^1 2s^0 2p^4$	2p	-11.9445	15.9076	-39.7854	15.1678	-3.2346	0.3433
			Total Energy = -164.0222				
$1s^1 2s^0 2p^3$	1s	-88.1701	97.9426	-197.9209	24.4631	-12.6549	0.0807
$1s^1 2s^0 2p^3$	2p	-14.5932	17.1338	-41.3353	12.8883	-3.2800	0.3273
			Total Energy = -152.2663				

TABLE VI (cont.)

$1s^1 2s^0 2p^2$	1s	-91.8374	98.2677	-198.2513	20.7353	-12.5891	0.0805
$1s^1 2s^0 2p^2$	2p	-17.4344	18.4041	-42.8732	10.3500	-3.3153	0.3126
			Total Energy = -137.8141				
$1s^1 2s^0 2p^1$	1s	-95.6747	97.8269	-197.8038	16.7563	-12.4541	0.0807
$1s^1 2s^0 2p^1$	2p	-20.4936	20.7229	-45.5187	7.7375	-3.4353	0.2914
			Total Energy = -120.4704				

TABLE VII Calculated H.F. binding energy, kinetic energy, nuclear interaction energy, electron-electron interaction energy in Rydbergs, and <r> in Angstroms for neon with configuration ($1s^0 2s^2 2p^n$).

Configuration	Shell	HF.B.E.	K.E.	N.I.E.	E.E.I.E.	EX.E.	<r> In Å
$1s^0 2s^2 2p^6$	1s	-84.0962	100.2018	-200.1927	29.2027	-13.3081	0.0797
$1s^0 2s^2 2p^6$	2s	-7.9964	14.6688	-38.4077	19.5362	-3.7938	0.4080
$1s^0 2s^2 2p^6$	2p	-6.1764	14.8546	-38.2046	20.7681	-3.5946	0.3716
			Total Energy = -120.3143				
$1s^0 2s^2 2p^5$	1s	-86.7814	100.4688	-200.4595	26.5061	-13.2969	0.0796
$1s^0 2s^2 2p^5$	2s	-9.9358	15.8496	-39.9076	17.8170	-3.6948	0.3921
$1s^0 2s^2 2p^5$	2p	-8.3945	16.1188	-39.9260	19.1093	-3.6965	0.3495
			Total Energy = -114.4980				
$1s^0 2s^2 2p^4$	1s	-89.8051	100.8232	-200.8132	23.4621	-13.2771	0.0794
$1s^0 2s^2 2p^4$	2s	-12.0499	17.1487	-41.4871	15.8635	-3.5750	0.3772
$1s^0 2s^2 2p^4$	2p	-10.8339	17.4085	-41.5823	17.1147	-3.7748	0.3311
			Total Energy = -106.4035				

TABLE VII (cont.)

$1s^0 2s^2 2p^3$	1s	-93.1546	101.2989	-201.2871	20.0821	-13.2485	0.0792
$1s^0 2s^2 2p^3$	2s	-14.3289	18.5395	-43.1119	13.6788	-3.4353	0.3634
$1s^0 2s^2 2p^3$	2p	-13.4851	18.6984	-43.1580	14.8049	-3.8303	0.3156
			Total Energy = -95.8182				
$1s^0 2s^2 2p^2$	1s	-96.8159	101.9604	-201.9436	16.3816	-13.2143	0.0789
$1s^0 2s^2 2p^2$	2s	-16.7648	19.9971	-44.7539	11.2696	-3.2777	0.3507
$1s^0 2s^2 2p^2$	2p	-16.3357	19.9454	-44.6162	12.1977	-3.8626	0.3025
			Total Energy = -82.5281				
$1s^0 2s^2 2p^1$	1s	-100.7630	102.8702	-202.8422	12.3898	-13.1808	0.0785
$1s^0 2s^2 2p^1$	2s	-19.3466	21.4697	-46.3602	8.6469	-3.1030	0.3389
$1s^0 2s^2 2p^1$	2p	-19.3695	21.1286	-45.9467	9.3214	-3.8729	0.2914
			Total Energy = -66.3308				
$1s^0 2s^2 2p^0$	2s	-22.0574	23.1869	-48.1654	5.8423	-2.9212	0.3269
			Total Energy = -47.0358				

TABLE VIII Calculated H.F. binding energy, kinetic energy, nuclear interaction energy, electron-electron interaction energy in Rydbergs, and <r> in Angstroms for neon with configuration ($1s^0 2s^1 2p^n$).

Configuration	Shell	HF.B.E.	K.E.	N.I.E.	E.E.I.E.	EX.E.	<r> in Å
$1s^0 2s^1 2p^6$	1s	-86.4209	99.3552	-199.3466	26.7474	-13.1769	0.0800
$1s^0 2s^1 2p^6$	2s	-10.0963	15.5085	-39.4858	17.7862	-3.9052	0.3959
$1s^0 2s^1 2p^6$	2p	-8.1083	15.9139	-39.6570	19.1545	-3.5197	0.3525
			Total Energy = -112.5913				
$1s^0 2s^1 2p^5$	1s	-89.3771	99.6664	-199.6587	23.7678	-13.1526	0.0799
$1s^0 2s^1 2p^5$	2s	-12.1919	16.7654	-41.0298	15.8666	-3.7941	0.3810
$1s^0 2s^1 2p^5$	2p	-10.5043	17.1957	-41.3151	17.2106	-3.5954	0.3339
			Total Energy = -104.7873				
$1s^0 2s^1 2p^4$	1s	-92.6581	100.0640	-200.0574	20.4528	-13.1175	0.0797
$1s^0 2s^1 2p^4$	2s	-14.4527	18.1197	-42.6281	13.7191	-3.6634	0.3672
$1s^0 2s^1 2p^4$	2p	-13.1129	18.5023	-42.9207	14.9566	-3.6511	0.3179
			Total Energy = -94.5430				

TABLE VIII (cont.)

$1s^0 2s^1 2p^3$	1s	-96.2531	100.5813	-200.5747	16.8124	-13.0721	0.0794
$1s^0 2s^1 2p^3$	2s	-16.8717	19.5504	-44.2554	11.3481	-3.5147	0.3544
$1s^0 2s^1 2p^3$	2p	-15.9256	19.8080	-44.4537	12.4068	-3.6866	0.3042
			Total Energy = -81.6455				
$1s^0 2s^1 2p^2$	1s	-100.1496	101.2879	-201.2785	12.8605	-13.0196	0.0791
$1s^0 2s^1 2p^2$	2s	-19.4424	21.0460	-45.8991	8.7613	-3.3506	0.3424
$1s^0 2s^1 2p^2$	2p	-18.9320	21.0630	-45.8702	9.5760	-3.7008	0.2924
			Total Energy = -65.8869				
$1s^0 2s^1 2p^1$	1s	-104.3279	102.3632	-202.3433	8.6257	-12.9734	0.0787
$1s^0 2s^1 2p^1$	2s	-22.1580	22.6333	-47.5879	5.9728	-3.1762	0.3307
$1s^0 2s^1 2p^1$	2p	-22.1112	22.1607	-47.0684	6.4874	-3.6908	0.2827
			Total Energy = -47.0657				
$1s^0 2s^1 2p^0$	2s	-24.9993	25.1769	-50.1762	3.0220	-3.0220	0.3159
			Total Energy = -24.9993				

TABLE IX Calculated H.F. binding energy, kinetic energy, nuclear interaction energy, electron-electron interaction energy, in Rydbergs, and <r> in Angstroms for neon with configuration ($1s^0 2s^0 2p^n$).

Configuration	Shell	HF.B.E.	K.E.	N.I.E.	E.E.I.E.	EX.E.	<r> in Å
$1s^0 2s^0 2p^6$	1s	-88.8561	96.9023	-196.8746	24.0682	-12.9520	0.0853
$1s^0 2s^0 2p^6$	2p	-10.1777	16.9598	-41.0179	17.2973	-3.4168	0.3369
			Total Energy = -102.7072				
$1s^0 2s^0 2p^5$	1s	-92.0579	97.0531	-197.0284	20.8183	-12.9009	0.0808
$1s^0 2s^0 2p^5$	2p	-12.7423	18.2589	-42.6266	15.0966	-3.4711	0.3207
			Total Energy = -92.7750				
$1s^0 2s^0 2p^4$	1s	-95.5694	97.2517	-197.2303	17.2441	-12.8349	0.0806
$1s^0 2s^0 2p^4$	2p	-15.5125	19.5809	-44.1900	12.6046	-3.5079	0.3065
			Total Energy = -80.2432				
$1s^0 2s^0 2p^3$	1s	-99.3781	97.5067	-197.4895	13.3575	-12.7628	0.0805
$1s^0 2s^0 2p^3$	2p	-18.4802	20.9076	-45.6951	9.8351	-3.5278	0.2940
			Total Energy = -64.9016				

TABLE IX (cont.)

$1s^0 2s^0 2p^2$	1s	-103.4554	97.7909	-197.7773	9.1832	-12.6522	0.0803
$1s^0 2s^0 2p^2$	2p	-21.6366	22.2637	-47.1760	6.8128	-3.5372	0.2824
			Total Energy = -46.5489				
$1s^0 2s^0 2p^1$	1s	-107.8146	99.9999	-199.9998	4.8560	-12.6706	0.0793
$1s^0 2s^0 2p^1$	2p	-24.9996	24.9999	-49.9995	3.6328	-3.6328	0.2645
			Total Energy = -24.9996				

Table X Total energy in Rydbergs and expectation value of r in Angstroms of all shells for various configurations of oxygen ($1s^{\ell}2s^{m}2p^{n}$).

Configuration ℓ	m	n	Total Energy	$\langle r \rangle_{1s}$	$\langle r \rangle_{2s}$	$\langle r \rangle_{2p}$
2	2	4	-149.4644	0.1053	0.6100	0.7194
2	2	3	-148.4101	0.1052	0.5873	0.6220
2	2	2	-146.0491	0.1051	0.5605	0.5592
2	2	1	-142.1495	0.1049	0.5344	0.5134
2	2	0	-136.4913	0.1046	0.5103	---
2	1	4	-147.1555	0.1052	0.5868	0.6203
2	1	3	-144.9019	0.1051	0.5616	0.5607
2	1	2	-141.1593	0.1050	0.5364	0.5158
2	1	1	-135.7077	0.1047	0.5116	0.4799
2	1	0	-128.3482	0.1051	0.4739	---

Table X (Cont.)

2	0	4	-143.4562	0.1052	---	0.5624
2	0	3	-139.8485	0.1050	---	0.5185
2	0	2	-134.5820	0.1048	---	0.4813
2	0	1	-127.4625	0.1052	---	0.4310
2	0	0	-118.1856	0.1061	---	---
1	2	4	-109.4180	0.1014	0.5470	0.5419
1	2	3	-106.6988	0.1013	0.5217	0.4940
1	2	2	-102.3136	0.1011	0.4977	0.4578
1	2	1	- 96.0443	0.1008	0.4759	0.4295
1	2	0	- 87.6870	0.1003	0.4564	0.4077
1	1	4	-105.5180	0.1014	0.5244	0.4975
1	1	3	-101.3276	0.1012	0.5009	0.4613
1	1	2	- 95.3033	0.1010	0.4790	0.4323
1	1	1	- 87.2365	0.1006	0.4582	0.4085
1	1	0	- 76.9210	0.1010	0.4291	---

Table X (Cont.)

1	0	4	- 99.9914	0.1013	---	0.4653
1	0	3	- 94.1873	0.1011	---	0.4358
1	0	2	- 86.3927	0.1008	---	0.4100
1	0	1	- 76.4092	0.1013	---	0.3739
1	0	0	- 63.9997	0.0992	---	---
0	2	4	- 61.9246	---	0.4949	0.4454
0	2	3	- 57.0569	---	0.4715	0.4162
0	2	2	- 50.1885	---	0.4503	0.3930
0	2	1	- 41.1129	---	0.4310	0.3740
0	2	0	- 29.6370	---	0.4118	---
0	1	4	- 56.0982	---	0.4777	0.4198
0	1	3	- 49.5127	---	0.4562	0.3955
0	1	2	- 40.7668	---	0.4365	0.3756
0	1	1	- 29.6559	---	0.4177	0.3596

Table X (Cont.)

0	0	4	- 48.4372	---	---	0.3992
0	0	3	- 39.9987	---	---	0.3780
0	0	2	- 29.2478	---	---	0.3590
0	0	1	- 15.9991	---	---	0.3306

Table XI Total energy in Rydbergs and expectation value of r in Angstroms of all shells for various configurations of nitrogen ($1s^{\ell}2s^{m}2p^{n}$).

Configuration			Total			
ℓ	m	n	Energy	$\langle r \rangle_{1s}$	$\langle r \rangle_{2s}$	$\langle r \rangle_{2p}$
2	2	3	-108.5268	0.1211	0.7108	0.8626
2	2	2	-107.6443	0.1210	0.6805	0.7280
2	2	1	-105.5907	0.1208	0.6447	0.6463
2	2	0	-102.1404	0.1204	0.6104	---
2	1	3	-106.7495	0.1210	0.6793	0.7242
2	1	2	-104.7967	0.1208	0.6460	0.6473
2	1	1	-101.4955	0.1206	0.6117	0.5902
2	1	0	- 96.6465	0.1212	0.5579	---

Table XI (Cont.)

2	0	3	-103.7421	0.1209	---	0.6488
2	0	2	-100.5709	0.1206	---	0.5913
2	0	1	- 95.9064	0.1213	---	0.5158
2	0	0	- 89.4353	0.1225	---	---
1	2	3	- 78.2943	0.1159	0.6232	0.6175
1	2	2	- 75.8891	0.1157	0.5906	0.5582
1	2	1	- 71.9562	0.1154	0.5604	0.5151
1	2	0	- 66.2863	0.1148	0.5336	---
1	1	3	- 75.0794	0.1159	0.5942	0.5622
1	1	2	-71.3357	0.1156	0.5643	0.5185
1	1	1	-65.9014	0.1152	0.5359	0.4841
1	1	0	- 58.5702	0.1157	0.4963	---

Table XI (Cont.)

1	0	3	- 70.4012	0.1157	---	0.5228
1	0	2	- 65.1838	0.1154	---	0.4858
1	0	1	- 58.1299	0.1161	---	0.4356
1	0	0	- 48.9998	0.1134	---	---
0	2	3	- 41.4299	---	0.5539	0.4961
0	2	2	- 37.0212	---	0.5248	0.4624
0	2	1	- 30.7561	---	0.4987	0.4358
0	2	0	- 22.4383	---	0.4733	---
0	1	3	- 36.4488	---	0.5328	0.4657
0	1	2	- 30.4582	---	0.5061	0.4380
0	1	1	- 22.4518	---	0.4810	0.4161

Table XI (Cont.)

0	0	3	- 24.7995	---	---	0.4411
0	0	2	- 22.0981	---	---	0.4154
0	0	1	- 12.2493	---	---	0.3778

APPENDIX B

CASCADE EFFECTS ON THE FLUORESCENCE YIELD

In this work we have presented explicit calculations to obtain the K-shell fluorescence yield, however, similar calculations could be performed for higher shells. For the K-shell, the experimental x-ray cross section, σ_K^x, is related to the ionization cross section, σ_K^i, by $\sigma_K^x = \omega_K \sigma_K^i$, where ω_K is the K-shell fluorescence yield. Extension of this relation to higher shells requires modification of the definition of the fluorescence yield. To illustrate, consider the L-shell. Coster-Kronig transitions are now possible. These are Auger transitions between the various L subshells. Explicitly, for the L-shell, these are the Auger transitions $L_1 - L_2 - X_\alpha$, $L_1 - L_3 - Y_\beta$, and $L_2 - L_3 - Z_\gamma$, where X_α, Y_β, and Z_γ represent any Auger electrons which are energetically possible. It is clear that these Coster-Kronig transitions can shift a primary vacancy in the L_1 or L_2 subshells to a vacancy in the L_3 subshell, with the simultaneous ejection of an M subshell Auger electron.

The extension of the relation between the x-ray cross section and the ionization cross section can be formulated most easily by defining a modified fluorescence yield, ν_{L_i}, equal to the ratio of the number of L x-rays produced to the number of primary vacancies in the L_i subshell. Further, we define the value of $f_{L_j L_k}$ as the probability of an L_j subshell vacancy being filled by an L_k subshell electron.

Consider the specific case of one vacancy in the L_1 shubshell. Then, the number of L_1 x-rays is equal to ω_{L_1} ; the number of L_2 x-rays is equal to $f_{L_1L_2}\omega_{L_2}$; and the number of L_3 x-rays is equal to $f_{L_1L_3}\omega_{L_3} + f_{L_1L_2}f_{L_2L_3}\omega_{L_3}$. The total number of x-rays for the L-shell is the sum of the number of x-rays for the individual L subshells, so the total number of L x-rays produced per L_1 vacancy is,

$$\nu_{L_1} = \omega_{L_1} + f_{L_1L_2}\omega_{L_2} + (f_{L_1L_3} + f_{L_1L_2}f_{L_2L_3})\omega_{L_3} . \quad (1)$$

Similarly, for an initial L_2 subshell vacancy, we have

$$\nu_{L_2} = \omega_{L_2} + f_{L_2L_3}\omega_{L_3} . \quad (2)$$

And, for an initial L_3 subshell vacancy, we have simply

$$\nu_{L_3} = \omega_{L_3} . \quad (3)$$

The relation between the x-ray production cross section and the inner shell ionization cross sections is

$$\sigma_L^x = \sigma_{L_1}^i \nu_{L_1} + \sigma_{L_2}^i \nu_{L_2} + \sigma_{L_3}^i \nu_{L_3}$$

where $\sigma_{L_1}^i$, $\sigma_{L_2}^i$, and $\sigma_{L_3}^i$ are the inner-shell ionization cross sections for the L_1, L_2, and L_3 shells respectively.

REFERENCES

1. Bergstrom and C. Nordling in Alpha, Beta, and Gamma-Ray Spectroscopy, Vol. II, 1523 (North-Holland Publishing Company, Amsterdam, 1965).

ACKNOWLEDGMENTS

It pleases me to express my appreciation to Dr. C.P. Bhalla who suggested the problem and has provided me with much assistance throughout this work.

Dr. N.O. Folland has taken part in many stimulating discussions, relative to this work, and has aided me constantly, for which I am earnestly thankful.

I am grateful to the U.S. Army Research Office of Durham, North Carolina, for their financial support, without which this project could not have been undertaken.

Finally, I want to extend my gratitude to my wife, Cheryl, for inspiration throughout this work.

K-SHELL AUGER AND X-RAY RATES, TRANSITION ENERGIES, AND FLUORESCENCE YIELDS FOR MULTIPLY IONIZED NEON, OXYGEN, AND NITROGEN

by

MICHAEL ANTHONY HEIN

B.S., University of Tulsa, 1969

AN ABSTRACT OF A MASTER'S THESIS

submitted in partial fulfillment of the

requirements for the degree

MASTER OF SCIENCE

Department of Physics

KANSAS STATE UNIVERSITY
Manhattan, Kansas

1973

ABSTRACT

The K-shell Auger rates, x-ray rates, fluorescence yields, and transition energies for multiply ionized configurations of neon, oxygen, and nitrogen are presented. Numerical calculations have been performed using a non-relatavistic Hartree-Fock-Slater model with the Herman-Van Dyke-Ortenburger exchange approximation. Comparisons of these explicit calculations with calculations based on the statistical model are reported. Differences up to 40% are shown for the fluorescence yield. Much higher differences, up to 80%, are found for the transition rates.